Journal of proteome research

ARTICLE

pubs.acs.org/jpr

Combined Proteomic and Metabolomic Profiling of Serum Reveals Association of the Complement System with Obesity and Identifies Novel Markers of Body Fat Mass Changes

Andreas Oberbach,[†,‡] Matthias Blüher,[†,§] Henry Wirth,[∥,⊥] Holger Till,[‡] Peter Kovacs,[#] Yvonne Kullnick,[†] Nadine Schlichting,[†,‡] Janina M. Tomm,[∥] Ulrike Rolle-Kampczyk,[¶] Jayaseelan Murugaiyan,[○] Hans Binder,[⊥] Arne Dietrich,[▽] and Martin von Bergen*[,∥,¶]

[†]IFB Adiposity Diseases, Leipzig University Medical Centre, Leipzig, Germany

[‡]Department of Pediatric Surgery, University of Leipzig, Leipzig, Germany

[§]Department of Medicine, University of Leipzig, Leipzig, Germany

[∥]Department of Proteomics, Helmholtz Centre for Environmental Research, Leipzig, Germany

[⊥]Interdisciplinary Centre for Bioinformatics, University of Leipzig, Leipzig, Germany

[#]Interdisciplinary Centre for Clinical Research, University of Leipzig, Leipzig, Germany

[¶]Department of Metabolomics, Helmholtz Centre for Environmental Research, Leipzig, Germany

[▽]Department of Visceral, Thoracic, Vascular and Transplant Surgery, University of Leipzig, Leipzig, Germany

[○]Institute of Animal Hygiene and Environmental Health, Freie University Berlin, Philippstr. 13, 10115 Berlin, Germany

Supporting Information

ABSTRACT: Obesity is associated with multiple adverse health effects and a high risk of developing metabolic and cardiovascular diseases. Therefore, there is a great need to identify circulating parameters that link changes in body fat mass with obesity. This study combines proteomic and metabolomic approaches to identify circulating molecules that discriminate healthy lean from healthy obese individuals in an exploratory study design. To correct for variations in physical activity, study participants performed a one hour exercise bout to exhaustion. Subsequently, circulating factors differing between lean and obese individuals, independent of physical activity, were identified. The DIGE approach yielded 126 differentially abundant spots representing 39 unique proteins. Differential abundance of proteins was confirmed by ELISA for antithrombin-III, clusterin, complement C3 and complement C3b, pigment epithelium-derived factor (PEDF), retinol binding protein 4 (RBP4), serum amyloid P (SAP), and vitamin-D binding protein (VDBP). Targeted serum metabolomics of 163 metabolites identified 12 metabolites significantly related to obesity. Among those, glycine (GLY), glutamine (GLN), and glycero-phosphatidylcholine 42:0 (PCaa 42:0) serum concentrations were higher, whereas PCaa 32:0, PCaa 32:1, and PCaa 40:5 were decreased in obese compared to lean individuals. The integrated bioinformatic evaluation of proteome and metabolome data yielded an improved group separation score of 2.65 in contrast to 2.02 and 2.16 for the single-type use of proteomic or metabolomics data, respectively. The identified circulating parameters were further investigated in an extended set of 30 volunteers and in the context of two intervention studies. Those included 14 obese patients who had undergone sleeve gastrectomy and 12 patients on a hypocaloric diet. For determining the long-term adaptation process the samples were taken six months after the treatment. In multivariate regression analyses, SAP, CLU, RBP4, PEDF, GLN, and C18:2 showed the strongest correlation to changes in body fat mass. The combined serum proteomic and metabolomic profiling reveals a link between the complement system and obesity and identifies both novel (C3b, CLU, VDBP, and all metabolites) and confirms previously discovered markers (PEDF, RBP4, C3, ATIII, and SAP) of body fat mass changes.

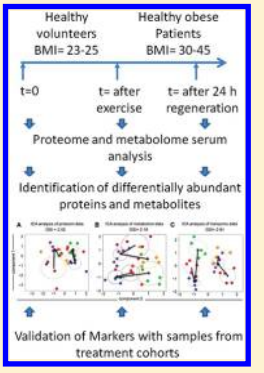

KEYWORDS: Proteomics, Metabolomics, obesity, bariatric surgery, weight loss therapy, lifestyle intervention

INTRODUCTION

Obesity has reached epidemic proportions worldwide.[1] It significantly increases the risk of developing type 2 diabetes mellitus, hypertension, coronary heart disease, stroke, and several types of cancer.[2] Adipose tissue releases a large number of bioactive molecules that influence body weight, insulin sensitivity, blood pressure, circulating lipids, coagulation, fibrinolysis and inflammation, leading to metabolic diseases as well as endothelial dysfunction and atherosclerosis. However, we are just beginning to understand the underlying mechanism that links increased fat mass to the adverse health outcomes of obesity.

Received: June 9, 2011
Published: August 09, 2011

During the past decade it has been realized that not only cells of the immune system and the liver but also adipose tissue expresses many pro- and anti-inflammatory factors and could therefore contribute to increased levels of inflammatory markers in the circulation of obese individuals.[3] Adipose tissue was shown to produce and secrete pro-inflammatory cytokines and adipokines including TNFα, transforming growth factor β (TGFβ) and interferon-γ, C-reactive protein (CRP), interleukins (IL) -1, -6, -8, -10, plasminogen activator inhibitor-1 (PAI-1), retinol binding protein-4 (RBP4), vaspin, fibrinogen, haptoglobin, angiopoietin-related proteins, metallothionein, complement factor 3, serum amyloid A (SAA) protein, anandamide and 2-AG as well as chemoattractant cytokines, such as monocyte chemotactic protein-1 (MCP-1), progranulin and macrophage inflammatory protein-1 as reviewed elsewhere.[2,4]

However, we hypothesize that important circulating factors, which may represent molecular mediators of increased risk for obesity-related diseases, are still unknown. Recent advances in proteomic and metabolomic approaches encourage studies that aim at identifying mechanisms underlying the pathophysiology of complex diseases such as obesity or diabetes as reviewed in refs 5 and 6. This study used a novel scientific approach in obesity research by combining proteome and metabolome data to identify molecules that discriminate healthy lean from healthy obese individuals.[7] Differentially abundant proteins were validated by ELISA. In addition, we measured serum concentrations of the identified proteins prior to and directly after exercise as well as 24 h after regeneration. Furthermore, we examined if significant loss of body fat mass in response to bariatric surgery or hypocaloric diet causes a change in the newly identified markers of fat mass.

The fact that serum protein concentrations vary by more than 15 orders of magnitude hampers the development of clinical biomarkers.[8] For our proteome study, we sought to exclude high abundant proteins and thus enable a higher coverage of the serum proteome by using a commercially available depletion kit that specifically immunoprecipitates 20 high abundant proteins from serum and that has been found to be compatible with other kits[9] and was used successfully in other studies.[10,11] Gel-based approaches allow the simultaneous detection of post-translational modifications and thereby the speciation of the proteome, whereas this information is often lost in peptide-based LC−MS approaches[12] that in contrast provide a much broader coverage of the proteome. Since until now the most accurate quantification in gel-based approaches is achievable by DIGE,[13] this technique was used in this study. The availability of high throughput analyses in the field of metabolomics is essential to cover metabolites important in lipid metabolism such as carnitine and phospholipids.[14] Functional analyses combined with a proteome approach have the potential for unraveling novel markers or mechanisms for pathophysiological conditions.[15] Furthermore, the detection of different metabolites is already used as a diagnostic tool in several diseases[16] including reproductive function,[17] insulin resistance[18] and consequences of laparoscopic sleeve surgery.[19] In recent studies, metabolome approaches have been used to either determine the differences between obese insulin resistant and sensitive patients[20] or metabolome footprints of diabetes, meaning the metabolome comparison between lean and diabetic individuals.[21] The metabolites covered in this study comprise a subset of those in the latter mentioned studies and include essential parts of the lipids correlated to obesity and adipose tissue.[21]

Serum proteins and metabolites exhibit a great variance due to short-term effects in the range of seconds up to 72 h, what is well-known as "metabolic adaptations." This metabolic adaptation is expected to be governed predominantly by the actual physical activity, nutrition and metabolism. To exclude the influence of short-term metabolic adaption, we used a one-hour physical exercise workout to create physical fatigue in the first step and regeneration afterward. Hence, measurements were taken at three points in time: baseline, immediately after the exercise and after 24 h of regeneration. This experimental design allowed us to (1) compare the circulating proteome and metabolome in response to acute exercise and (2) dissect those proteins or metabolites that may reflect individual differences in fat mass, independently of physical activity status. Only those proteins and metabolites, which independently of exercise-associated changes predict fat mass, were considered for further analyses in the context of two weight loss intervention strategies. We sought to determine whether changes in the identified proteins and metabolites 6 months after either bariatric surgery or an energy restricted diet are correlated with changes in fat mass.

MATERIAL AND METHODS

Ethic Statement

The study protocols were approved by the University of Leipzig ethic committee review board, and all subjects provided their informed consent before entering the study.

Study Design

Combined Proteome and Metabolome Study in Healthy Lean vs Obese Individuals. In a cross-sectional exploratory study, 5 healthy lean and 5 healthy obese Caucasian (all males; Table S1, Supporting Information) were randomly selected, out of a cohort of 15 healthy lean and 15 healthy obese volunteers (Table 1), to identify serum biomarkers via 2D DIGE. The identified markers were later on validated by a comparison of 15 lean and 15 obese individuals selected by the same criteria as the smaller group based on ELISA analysis. The volunteers were selected from a computer-based volunteer database and matched for age and health status. All individuals fulfilled the following inclusion criteria: (1) age 20−35 years, (2) BMI 23−25 kg/m^2 (lean group) or 30−45 kg/m^2 (obese group), (3) fasting plasma glucose < 6.0 mmol/L, (4) HbA1c < 5.5%, and (5) stable weight, defined as the absence of fluctuations of 2% of body weight 3 months before the study. In addition, the following exclusion criteria have been defined: (1) medical and family history of type 1 or type 2 diabetes, (2) medical history of hypertension or systolic blood pressure (SBP) 140 mmHg and diastolic blood pressure (DBP) 85 mmHg, (3) any acute or chronic inflammatory disease, as determined by a cardiovascular or peripheral artery disease, (4) any type of malignant disease, (5) thyroid dysfunction, (6) Cushing's disease or hypercortisolism, (7) alcohol or drug abuse, (8) pregnancy, (9) concomitant medication, (10) leukocyte count < 8000 Gpt/L, and (11) C-reactive protein (CRP) > 5.0 mg/L. All subjects completed a graded bicycle test to volitional exhaustion and had maximal oxygen uptake measured with an automated open circuit gas analysis system at baseline. The highest oxygen uptake per minute was defined as the maximal oxygen uptake (VO_2 maximum).

Acute Exercise Bout Study. *Exercise Protocol.* All subjects from the combined proteome and metabolome study participated in an acute exercise bout. Ten healthy males completed

Table 1. Characteristics of Lean (n = 15) and Obese (n = 15) Volunteers[a]

	lean (n = 15)		obese (n = 15)		
variable	mean (SD)	range	mean (SD)	range	p-value
Age [years]	23.7 (±1.99)	20−27	24.1 (±3.11)	20−30	
BW [kg]	81.0 (±9.68)	69.1−106.6	120.4 (±22.2)	90.9−175.5	0.0001
Height [cm]	184.4 (±6.76)	170.1−196.7	179.8 (±6.86)	168.5−191.2	
BF [%]	14.5 (±3.69)	9.8−19.3	40.8 (±3.88)	35.6−49.3	0.0001
BMI [kg/m^2]	23.8 (±1.77)	21.1−27.8	37.3 (±7.21)	28.3−55.8	0.0001
FPG [mmol/L]	5.0 (±0.54)	4.3−6.0	4.8 (±0.55)	3.7−5.8	0.596
HbA1C [%]	4.7 (±0.0.25)	4.2−5.1	4.8 (±0.23)	4.3−5.3	0.433
FPI [pmol/L]	57.29 (±9.1)	43.1−61.3	62.12 (±6.71)	46.3−68.3	0.109
2-h OGTT plasma glucose [mmol/L]	5.07 (±0.17)	4.8−5.4	5.09 (±0.26)	4.8−5.5	0.804
Triglycerides [mmol/L]	1.75 (±1.02)	0.83−4.55	1.95 (±1.14)	1.01−4.55	0.618
Total-cholesterol [mmol/L]	5.6 (±1.54)	4.8−8.1	5.8 (±0.99)	4.1−7.2	0.676
HDL-cholesterol [mmol/L]	1.74 (±0.55)	1.14−1.4	1.39 (±0.47)	0.63−2.25	0.074
hsCRP [mg/L]	2.77 (±0.33)	2.21−3.29	2.77 (±0.25)	2.34−3.13	0.98

[a] P-values are presented using unpaired Student t-test.

one 60-min resistance circuit training at 80% of individual maximal power. The training sessions consisted of three repetitions at different stations with 30 s break time (Figure S1A, Supporting Information). At baseline, immediately and 24 h after exercise blood samples were taken in the fasting state. All baseline and postintervention blood samples were collected between 8:00 and 10:00 a.m. after an overnight fast.

Intervention Studies. In two different intervention studies (hypocaloric diet study and bariatric surgery study), we evaluated the association of changes of potential biomarkers with changes of fat mass and parameters of glucose homeostasis. To compare the biomarkers with age-, gender- and BMI-matched controls, we used 17 healthy subjects out of our volunteer database. The control subjects fulfill the following inclusion criteria: (1) age 35−60 years, (2) BMI 23−30 kg/m^2, (3) fasting plasma glucose < 7.0 mmol/L, (4) HbA1c < 5.5%, and (5) stable weight, defined as the absence of fluctuations of 2% of body weight 3 months before the study. Furthermore, the above-mentioned exclusion criteria have been applied to the control group.

Six Months Hypocaloric Diet Study. Twelve Caucasian obese subjects (6 females, 6 males) attending the Obesity Outpatients Clinic at the University of Leipzig Medical Department were recruited. Patients underwent a clinical assessment including medical history, physical examination, DEXA scan analysis, comorbidity evaluation as well as nutritional interviews performed by a multidisciplinary consultation team. All individuals fulfilled the following inclusion criteria: (1) fasting plasma glucose < 6.0 mmol/L, (2) HbA1c < 6.0%, and (3) stable weight, defined as the absence of fluctuations of >2% of body weight for at least 3 months. In addition, the following exclusion criteria have been defined: (1) medical and family history of type 1 or type 2 diabetes, (2) medical history of hypertension or systolic blood pressure (SBP) > 140 mmHg and diastolic blood pressure (DBP) > 85 mmHg, (3) any acute or chronic inflammatory disease as determined by a leukocyte count >8000 Gpt/l, C-reactive protein (CRP) > 5.0 mg/L or clinical signs of infection, (4) clinical evidence of either cardiovascular or peripheral artery disease, (5) any type of malignant disease, (6) thyroid dysfunction, (7) Cushing's disease or hypercortisolism, (8) alcohol or drug abuse, (9) pregnancy, and (10) concomitant medication except contraceptives. Weight loss was achieved over a period of 6 months by a diet providing a daily energy deficit of 1200 kcal/d (Figure S1B, Supporting Information).

Bariatric Surgery Study. Fourteen Caucasian obese subjects (9 females, 5 males) participated in a prospective weight loss study before and 6 months after gastric sleeve resection. The baseline BMI was 54 ± 8 kg/m^2 and the BMI 6 months after bariatric surgery was 36.3 ± 7.3 kg/m^2. Individuals fulfilled the following exclusion criteria: (1) presence of any malignant, acute or chronic inflammatory disease as determined by a leukocyte count >7000 Gpt/l, C-reactive protein (CRP) > 5.0 mg/L or clinical signs of infection, (2) detectable antibodies against glutamic acid decarboxylase (GAD), (3) clinical evidence of either cardiovascular or peripheral artery disease, (4) thyroid dysfunction, (5) alcohol or drug abuse, and (6) pregnancy.

Measures of Body Fat Content, Oral Glucose Tolerance Test, and ELISA-Assays

Measures of Body Fat Content. Body mass index (BMI) was calculated as weight divided by squared height. Hip circumference was measured over the buttocks; waist circumference was measured at the midpoint between the lower ribs and iliac crest (Figure S1B, Supporting Information). Percentage body fat was measured by dual X-ray absorptiometry (DEXA).

Oral Glucose Tolerance Test. Three days before the oral glucose tolerance tests (OGTT) patients documented a high-carbohydrate diet. The OGTT was performed after an overnight fast with 75 g of standardized glucose solution (Glucodex Solution 75 g; Merieux, Montreal, Canada). Venous blood samples were taken at 0, 60, and 120 min for measurements of plasma glucose concentrations. All baseline blood samples were collected between 8:00 and 10:00 a.m. after an overnight fast. All baseline blood samples were collected in S-Monovette for serum and plasma (Sarstedt, Nümbrecht, Germany) between 8:00 and 10:00 a.m. after an overnight fast. After centrifugation, the aliquots were stored in 2 mL cryovials (VWR, Darmstadt, Germany) in liquid nitrogen until processing. No further additives such as anticoagulants, preservatives, and protease inhibitors were used. The blood samples were centrifuged immediately after collection (10 min, 4 °C, 2500× g) and separated into aliquots as described above. Fasting plasma insulin was measured with an enzyme immunometric assay for the IMMULITE-automated

dx.doi.org/10.1021/pr2005555 |J. Proteome Res. 2011, 10, 4769–4788

analyzer (Diagnostic Products Corporation, Los Angeles, CA). The HbA1c values were determined with a cation exchange/high-performance liquid chromatography method (reference values 3.4−6.0%). Serum high-sensitive CRP was measured by immunonephelometry (Dade-Behring, Milan, Italy). Serum total-, HDL-cholesterol and triglycerides were measured as previously described (Kloting et al., 2007).

ELISA Assays. Quantitative ELISA assays for evaluation of detected proteins by MS/MS. Proteome validation studies were performed using the following immunoassays: Quantikine human vitamin D-binding protein immunoassay (R&D Systems, Minneapolis, MN), Quantikine human RBP4 immunoassay (R&D Systems), human PEDF ELISA (BioVendor, Heidelberg, Germany), Human clusterin ELISA (BioVendor), ELISA kit for human serum amyloid P-component (Uscn Life Science Inc. Wuhan, China), ELISA kit for human complement component 3 (Uscn Life Science Inc. Wuhan), Quidel iC3b EIA kit (Quidel Corporation, San Diego, CA), AssayMax human high molecular weight kininogen 1 ELISA kit (Assaypro, St. Charles, MO) and AssayMax human antithrombin III ELISA kit (Assaypro). All immunoassays were performed according to the manufacturer's recommendations. Complement functional activities of classical, alternative and mannose binding lectin (MBL) pathways were measured with Wieslab complement system screen enzyme immunoassay (Euro-Diagnostica AB, Malmö, Sweden) described by ref 22. The Wieslab complement assay combines principles of the hemolytic assay for complement activation with the use of labeled antibodies specific for neoantigen produced as a result of complement activation. The wells of the microtiter strips were coated with specific activators of the classical (IgM), the alternative (LPS), or the MBL pathway (mannan). Sera were diluted in specific blocking buffer to ensure that only the respective pathway is activated. C5b-9 was detected with a specific alkaline phosphatase-labeled antibody to the neoantigen expressed during formation of membrane attack complex. Detection of specific antibodies was obtained by incubation with alkaline phosphatase substrate solution. The amount of complement activation correlates with the color intensity and was measured in terms of absorbance (optical density, OD = 405 nm). The negative controls (NC) and positive controls (PC) were used in a semiquantitative way to calculate complement activity. After calculation of the mean OD405 nm values for serum samples, PC and NC the % complement activity was calculated as follows: (Sample − NC)/(PC − NC) × 100.

Serum Preparation for Proteome Analysis

High-Abundance Protein Depletion. Twenty high-abundance proteins were depleted from plasma using the ProteoPrep 20 Plasma Immunodepletion Kit (Sigma Aldrich, Steinheim, Germany). Immunodepletion spin columns with 300 μL of packed medium were used for depleting 100 μL of diluted plasma (dilution 1:12.5 with equilibration buffer). Concentration of multiple depletions was carried out using Ultrafree-MC Microcentrifuge Filters (NMWL 5000 Da). Protein concentration of whole and depleted plasma was determined using the Bradford Reagent (Sigma Aldrich) with BSA as standard.

Sample Preparation for 2D Gels. One-hundred micrograms of serum protein (low abundance proteins) were acetone precipitated as described elsewhere.[23] The precipitate was reconstituted with labeling buffer, pH 9.0 (7 M Urea, 2 M Thiourea, 4% CHAPS, 30 mM Tris). Solubilization of the precipitate was facilitated by sonication for 30 s and the pH of the solution was adjusted to pH 8.5. The precipitates were then labeled using the fluorescent cyanine dyes according to the minimal labeling protocol of the manufacturer (GE Healthcare, Munich, Germany). The internal standard was prepared by pooling equal proteins of each of the ten serum samples and this standard was then labeled with 200 pmol of Cy2 dye per sample. The remaining volume from lean or obese patients was labeled with 200 pmol of either Cy3 or Cy5 dye. For the labeling reaction, the samples with Cy dyes were incubated for 30 min on ice in the dark. The reaction was quenched by the addition of 1 μL of 10 mM lysine, was vortexed, and was left for another 10 min on ice in the dark. The quenched Cy3- and Cy5-labeled samples and the Cy2-labeled internal standard were pooled. Half of a microliter of this mixture was taken for running SDS-PAGE to verify the efficiency of DIGE labeling procedure; 370 μL of DeStreak buffer (GE Healthcare) was then added to each Cy-labeled sample pool, vortexed and centrifuged at 13 000 rpm for 30 min at 20 °C. This protein solution was applied immediately onto an Immobiline IPG Dry Strip, pH 4−7, 24 cm (GE Healthcare), as described below.

IEF and Gel Electrophoresis. Immobiline dry strips (pH 4−7, 24 cm, GE Healthcare) were rehydrated for 12 h in dark. The IPG strips were then focused using an Ettan IPGPhor 3 IEF system (GE Healthcare) as described previously.[24] In brief, the stripes were focused at 500 V for 1 h, 1000 V for 7 h, and at 8000 V for a total of 110 000 VhT at 20 °C. Each gel strip was equilibrated twice, 15 min each time, with equilibration buffer (6 M urea, 30% glycerol, 2% SDS, 50 mM Tris-HCl, pH 8.8) containing first 1% w/v DTE and then 2.5% w/v iodoacetamide and a pinch of bromophenol blue. The equilibrated strips were then carefully placed on top of 12% acrylamide gels and sealed with 1% w/v agarose. Second dimension separations were performed on an Ettan DALTtwelve electrophoresis system (GE Healthcare). The proteins were separated initially at 12 °C, 1 W/gel for 12 h, followed by 12 W/gel until the dye front reached the bottom of the gel. During all stages, work was carried out with great care to avoid its exposure to light.

Image Acquisition and Data Analysis of 2D Gels. Immediately after the run, DIGE gels were scanned within the gel cassettes using Ettan DIGE Imager Scanner (GE Healthcare). The Cy2 dye was excited at 488 nm and emission spectra were obtained at 520 nm, the Cy3 dye was excited at 532 nm and emission spectra were obtained at 580 nm, and the Cy5 dye was excited at 633 nm and emission spectra were obtained at 670 nm. The gels were visualized and first evaluated with the Image Quant Software, whereby all the three images as well as an overlay image of these images were checked individually. After scanning, the gels were removed from the gel cassette and were stained overnight with blue silver staining procedure. DIGE gel analysis was performed with Delta2D 3.6 software (Decodon, Greifswald, Germany) with advanced image processing algorithms that permits image fusion using internal standards, background subtraction, normalization, and relative quantitation of proteins from different images. Following automated spot detection, each spot was manually verified and edited using 3D view algorithm. Differentially expressed spots were identified after filtering the 0.5−2.0% ratio volume of the spots on different gels. Furthermore, p-value was set at <0.05 in all statistical group comparisons. Only these spots were given an identification number for further analysis.

In-Gel Digests and Sample Preparation. Protein spots of interest were cut from polyacrylamide gels and digested

overnight using trypsin as described elsewhere.[25] The spots were washed two times with water/acetic acid/ethanol (50:5:45 v/v) for one hour. The gel spots were shrunk by the addition of acetonitrile, reduced and alkylated with DTT and Iodoacetamide. Afterward, the gel slices were incubated with 5 mM ammonium bicarbonate, followed by incubation with acetonitrile 100% and dried by vacuum centrifugation. The dried gel pieces were swollen by adding trypsin in ammonium carbonate buffer (100 mM, pH 8.5) and were incubated at 37 °C for 12 h. Extractions of peptide were performed with extraction buffer containing acetonitrile/water/formic acid (5: 4.4:0.6 v/v). The extracted peptide solutions were then completely dried using vacuum centrifugation. After that, the precipitates were reconstituted with 10 μL of 5% acetonitrile in 0.1% trifluoroacetic acid; 0.5 μL of this peptide extract and 0.5 μL of HCCA were mixed and spotted on ground steel target plates (Bruker Daltonics, Bremen, Germany).

Protein Identification

Protein Identification by MALDI-MS/MS. Peptide identification was carried out with MALDI-TOF MS/MS (Ultra Flex III TOF/TOF, Bruker Daltonics, Bremen, Germany) using ground steel MTP 384 target plate (Bruker Daltonics) according to the manufacturer's instructions. In brief, the samples were prepared by mixing equal volumes (1 μL) of sample and HCCA matrix (0.1 g/L of α-Cyano-4-hydroxycinnamic acid) and were then spotted onto the ground steel MTP 384 target plate. The solution was allowed to evaporate at room temperature. Spectra were obtained on an MALDI-TOF/TOF mass spectrometer (Ultraflex III, using FlexControl software Vs. 3.0; Bruker Daltonics) as described earlier.[25] In brief, the instrument was operated at pulse rates of 100 Hz; pulse ion extraction delay was set to 400 ns as described earlier.[26] Measurements were carried out in positive reflector mode using an acceleration voltage of 25.0 kV (ion source 1) and 21.85 kV (ion source 2). Lens voltage was 9.5 kV, reflector voltages were 26.3 and 13.7 kV. Mass spectra were recorded in the m/z range between 200 and 3500. If possible, up to 10 MS^2 spectra were performed. The spectra were processed by the software FlexAnalysis (Bruker Daltonics). Thereafter, a database search was conducted using the MS/MS ion search (MASCOT, Matrix Science, London, U.K.; version 2.2) against all metazoan (animals) entries of NCBInr (GenBank) with subsequent parameters trypsin digestion, up to one missed cleavage; fixed modifications carbamidomethyl (C); and with the following variable modifications, oxidation (M), peptide tol. ± 1.2 Da, MS/MS tol. ± 0.6 Da, peptide charge +1, +2 and +3.

Protein Identification by Nano-LC−ESI−MS/MS. In cases of ambiguous identifications and for all validated proteins, the identification was repeated by measurement by LTQ-Orbitrap-MS (Thermo Fisher Scientific, San Jose, CA). In-gel digestion samples were injected and concentrated on a trapping column (nanoACQUITY UPLC column, C18, 180 μm × 2 cm, 5 μm, Waters, Eschborn, Germany) with water containing 0.1% formic acid at flow rates of 15 μL/min as described in ref 27. Peptides were eluted onto a separation column (nanoACQUITY UPLC column, C18, 75 μm × 250 mm, 1.7 μm, Waters) and separation was done over 30 min with a 2−40% solvent B gradient (0 min, 2%; 2 min, 8%; 20 min, 20%; 30 min, 40%). Scanning of eluted peptide ions was carried out in positive ion mode in a range m/z 350−2000, automatically switching to CID-MS/MS mode on ions exceeding an intensity of 2000. For CID-MS/MS measurements, a dynamic precursor exclusion of 3 min was applied. Proteins were identified by database search using MASCOT (MASCOT (Matrix Science, London, U.K.; version 2.2) and SEQUEST (Thermo Fisher Scientific, San Jose, CA; version 1.0.43.0).

Targeted Metabolomics

Targeted metabolite profiling by electrospray ionization (ESI) tandem mass spectrometry (MS/MS) was performed at Biocrates Life Sciences AG, Austria (http://www.freepatentsonline.com/20070004044.html). Briefly, a targeted profiling scheme was used to quantitatively screen for 163 metabolites using multiple reaction monitoring, neutral loss and precursor ion scans. The quantification of the metabolites of the biological sample was achieved by reference to appropriate internal standards. The method is proven to be in conformance with 21CFR (Code of Federal Regulations) Part 11 and has been used successfully in the past in various applications.[14,15,21]

Statistical Analysis

The abundance of proteins and metabolites was measured by means of 2D-DIGE and targeted ESI-MS, respectively, as described above. It is quantified in units of relative abundance in relation to the respective reference marker. Differences between the two groups (lean and obese, group size =5) at the three different times of treatment ("pre", "post" and "24h") were determined using the two sample t test. It is applied to the logged abundance data, which distribute normally to a good approximation (data not shown). The significance level was set at $p < 0.05$. The false discovery rate (FDR) was estimated as a function of p from the distribution of p-values using the software fdr-tool.[28] For the proteins and metabolites we obtained FDR = 0.25 and 0.35 at the significance level, respectively. Hence, between about one-fourth and one-third of the selected features are supposed to be false positives. For a more strict selection, only features which are significantly different at all three treatment times are considered for downstream analysis. These features are assumed to reflect the difference between lean and obese test persons, independent of their physical conditioning (see Venn-diagram in Figure 2C group comparison).

Parameters significantly changing with time were detected for lean and obese persons using analysis of variance (ANOVA) with a significance threshold of $p < 0.05$. Prepost comparisons in the two intervention studies have been performed using student's t test. $P < 0.05$ was considered as significant. Multiple linear regression analyses have been performed to test whether identified parameters predict changes in body fat mass independently of other factors including weight, BMI, HbA1c, etc. Only parameters with significant differences between lean and obese in at least one of the three conditions are selected to focus on differential features between the test groups (see Venn diagram in Figure 2C for time comparison). Volcano plots of the logged p-value as a function of the logged fold change (FC) are used to visualize the test results. It should be noted that p-values might fall below the significance threshold for vanishing logFC values in this representation in contrast to Volcano plots representing the results of paired t tests.[29] Selected proteins were assigned to functionally related sets and pathways of proteins using the GENE CARDS database[30] (Figure 1 and Figure S2, Supporting Information).

Independent Component Analysis and Pairwise Correlation Maps

Independent component analysis (ICA) was performed to visualize the similarity of selected features between the test groups at different conditions.[31] This method decomposes

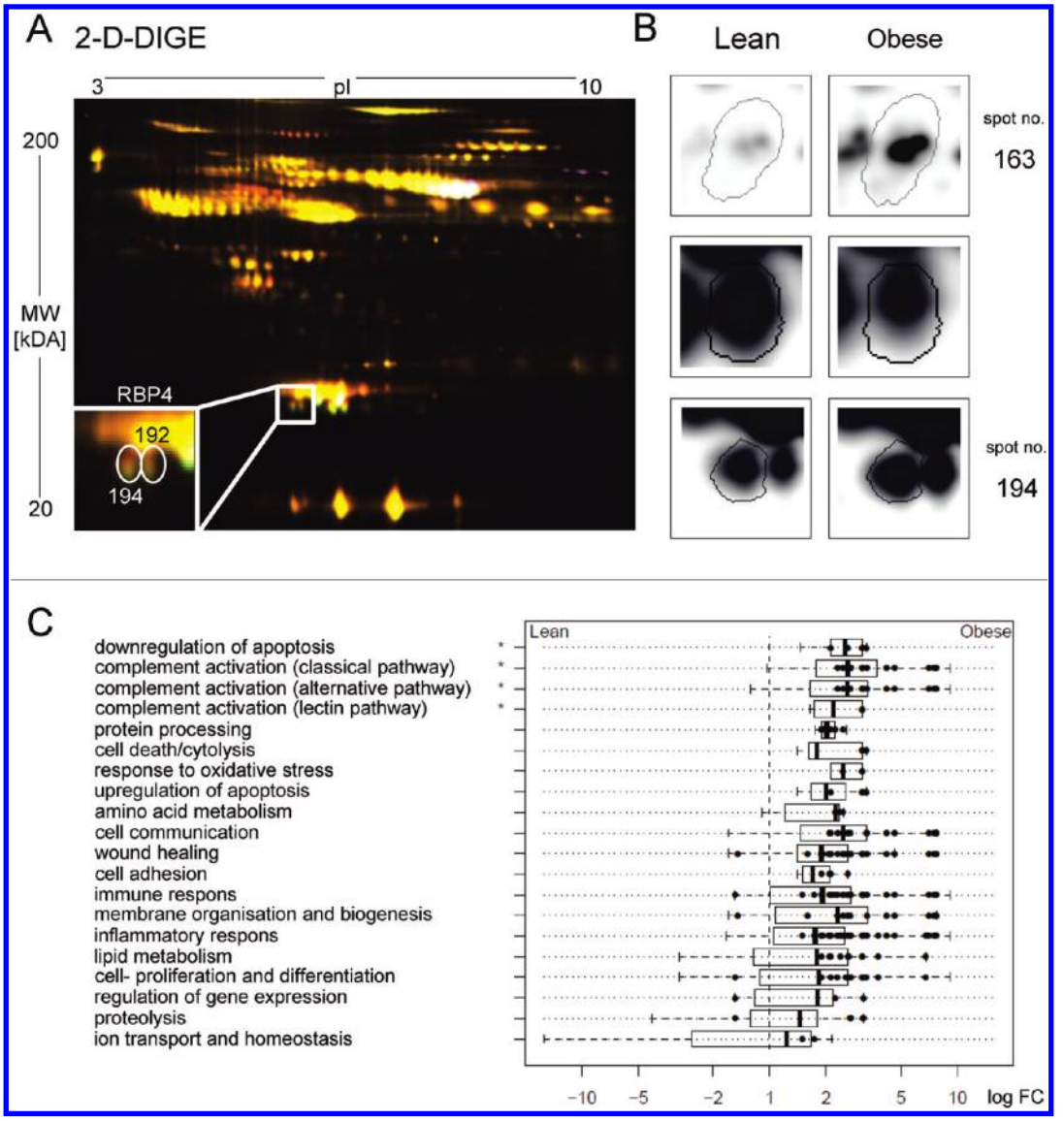

Figure 1. DIGE of serum proteome reveals pathways regulated in obesity. (A) Gel displays a representative example of serum from a lean volunteer. (B) Quantification of selected spots and area maps of C3, C3b and RBP4. (C) Pathway related gene enrichment is shown by values (black circles) of fold changes from regulated proteins annotated to the various pathways. The pathway cumulated *p*-values are calculated and significantly enriched pathways ($p < 0.05$) are marked by asterisks.

multivariate data sets into statistically independent components of variance. ICA enables efficient decomposition of non-Gaussian data distributions in contrast to Principal Component Analysis (PCA), which efficiently applies only to Gaussian variables. Application of ICA to metabolomics, proteomics and combined data sets is more informative than PCA as has been demonstrated previously[32] mainly due to this fact. The ICA plots show each sample in the coordinates of the two topmost independent components. Different samples will arrange in parallel to one of the ICA-axis if their behavior is governed by dependent features and in perpendicular direction if the respective features change independently. ICA was separately applied to metabolomics and proteomics data and to a combination of both data sets as well. The individual features of this integrated "transomic" data set were transformed into *z* scores, $z = (x - m)/\sigma$, before ICA analysis. x and m denote the individual feature and its mean over the replicates in logarithmic scale with σ as respective standard deviation. We defined the normalized *group separation index* (GSI) to assess the power of each data set discriminating between the experimental groups (obese versus lean and time-dependent effects) in ICA-coordinates as GSI = (mean distance between the samples of different groups)/(mean distance between the samples of the same group). The separation between the groups and thus the classification power of the respective data increase with the GSI-value as illustrated in Figure 5. Each experimental group is coded by one color. Full and open dots assign the individual measurements and the group centroids, respectively. The dashed and the dotted circle indicate the mean intragroup and intergroup distances, respectively.

In addition to ICA, we generated pairwise correlation maps (PCM) to visualize the Pearson correlation coefficients of the molecular profiles in all pairwise combinations of samples. PCM were calculated separately for metabolomics and proteomics data and for the integrated "transomics" data set in analogy to the ICA

dx.doi.org/10.1021/pr2005555 |*J. Proteome Res.* 2011, 10, 4769–4788

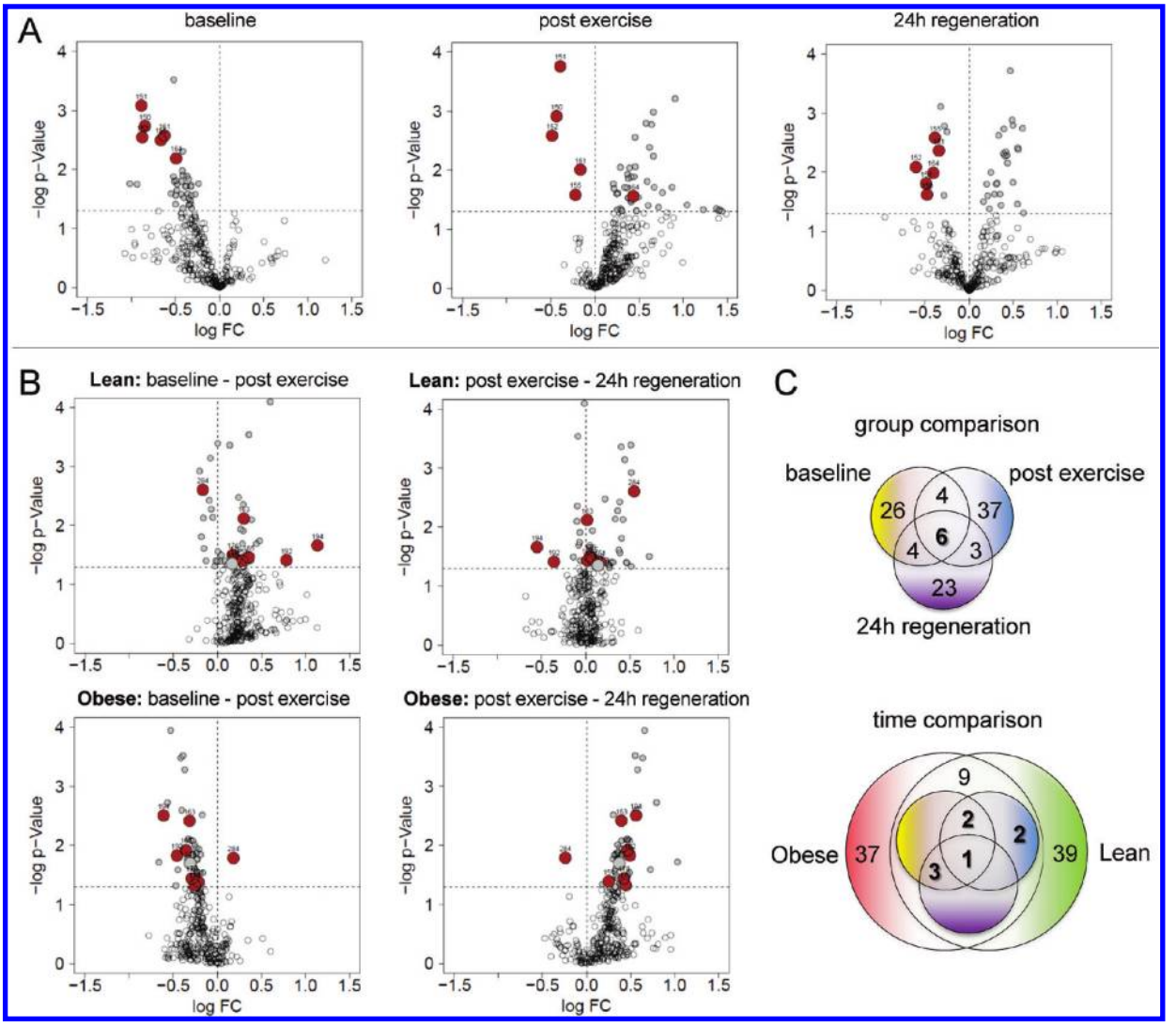

Figure 2. Serum protein fingerprint from healthy lean and obese subjects. The relative changes in abundance of proteins are displayed as Vulcano plots for (A) group dependant comparisons and (B) time comparisons. Minus log fold-change (FC) in A indicate upregulation in obese subjects. The horizontal dotted line represents the significance threshold ($p < 0.05$) and the significantly regulated proteins are highlighted in red. The results are summarized as (C) Venn diagram exhibiting the commonly and specifically affected proteins.

analysis. PCM heat map visualization is combined with hierarchical clustering to estimate mutual similarities between the samples.

Pathway Analysis

Selected proteins were associated with concepts of molecular and physiological function and assigned to functional sets of proteins making use of the GENE CARDS database as described in Henegar et al.[30] Set-wise averaging of the logged FC values over the set members provides estimates of the set-related overexpression and of the respective standard error, which allows interpretation of concerted changes of protein abundance in a functional context (see ref 33). Fold changes of members of each set in pairwise comparison between lean and obese test persons are shown as box plots indicating the median as well as the 25 and 75% interquartile ranges (Figure 1 and Figure S2, Supporting Information). Set members with significant fold changes in their abundance were presented separately by filled circles in Figure 1D (Table S5, Supporting Information). The *p*-value, which has been obtained from averaged *t*-scores of all set members, allows us to estimate the significance of the observed fold changes of each set (threshold $p = 0.05$).

Comparison of Treatments

Baseline-post fold changes of selected markers are compared in nutrition and surgery treatments in study 2 using appropriate correlation plots. The significance of the FC-values was estimated by means of the *t* test with a significance threshold of $p = 0.05$. Further, multiple linear regression was applied to estimate the effect of selected clinical factors (Table 1). This model assumes a linear relation between the molecular and clinical markers. The obtained regression coefficients ("beta"-coefficients) estimate the statistical weight of each clinical marker in the linear combination of all markers.

RESULTS

Identification of 4 Proteins as Exercise-Independent and 7 Proteins as Exercise Dependent Predictors of Fat Mass Differences in Healthy Individuals

Combined serum proteome and metabolome analyses were performed in five lean and five obese healthy young men, which have been matched for age and health status (Table S1,

dx.doi.org/10.1021/pr2005555 |J. Proteome Res. 2011, 10, 4769–4788

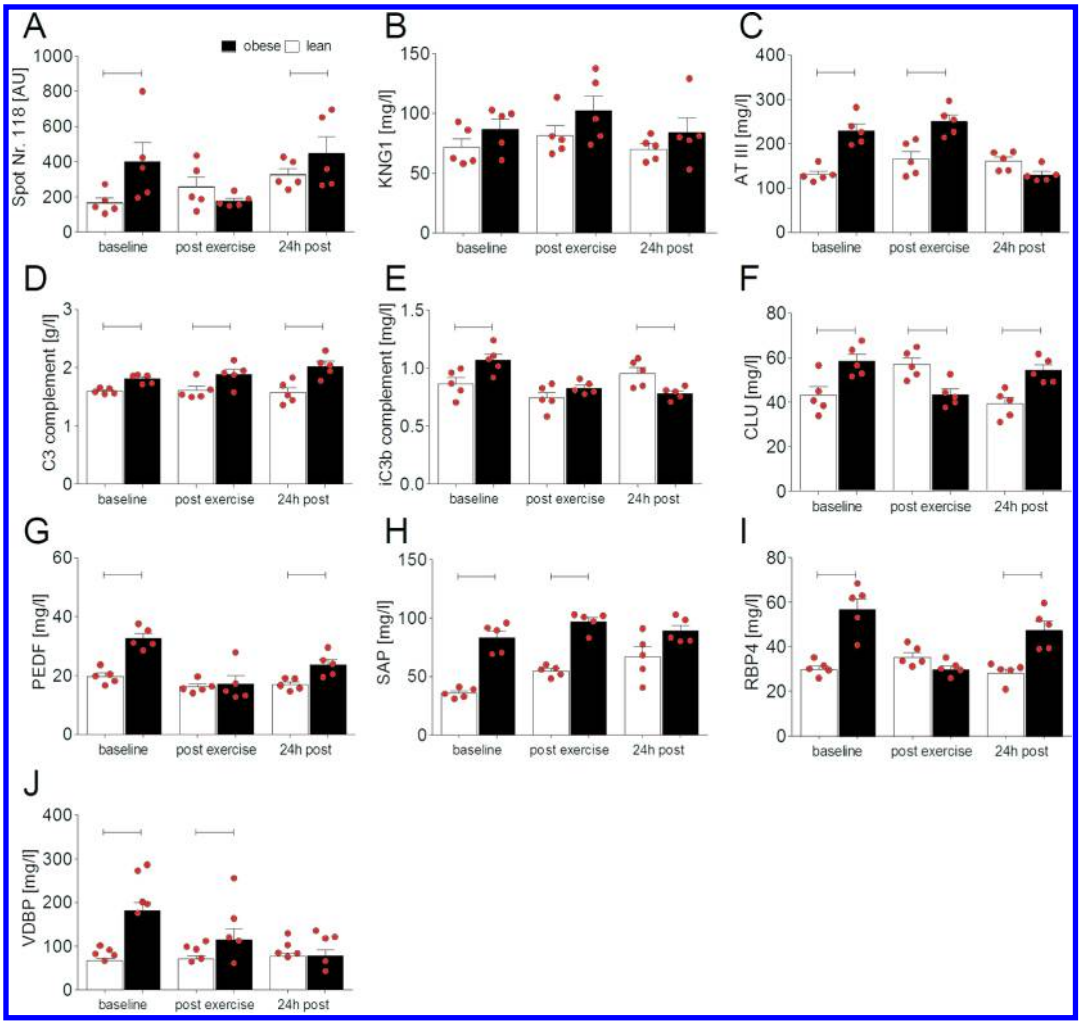

Figure 3. Validation of differentially expressed proteins by ELISA. On the basis of spot density, (A) significant regulation of spot 118 was found, the identification yielded (B) KNG1 and (C) SERPINC1 with significant scores. The ELISA of both KNG1 and SERPINC1 evaluated SERPINC1 as the most relevant affected protein (C). ELISA data from C3, IC3b, CLU, PEDF, APCS, RBP4 and VDBP are shown as means with SEM in D−J. White bars represent lean, black bars indicate obese subjects. Every single value is shown as red circle. Lines above bars indicate significant ($p < 0.05$) changes between groups using unpaired Student *t* test.

Supporting Information). To exclude exercise-dependent circulating protein changes, the serum proteome was analyzed at three points in time: at baseline, immediately after a one-hour exercise bout and after 24 h of regeneration (Figure S1A, Supporting Information). Only those proteins were taken into account that significantly differ either at all three points between the two groups (group effect) or between the points in time independent of the obesity status.

The depletion of 20 high abundant proteins from the serum, including albumin, resulted in gels resolving up to 289 protein spots (Figure 1A) from which 135 spots were detectable for all of the conditions studied (Table S2, Supporting Information). To allow a quantitative analysis of affected pathways all spots were subjected to protein identification so that the number of proteins belonging to certain pathway was used as normalization since the affected spots were determined. Only 6 out of these 126 spots (Table S3, Supporting Information, Figure 2A) showed significant differences between lean and obese individuals at all points in time (Figure 2A and C group comparison). These spots are assigned to four different proteins (Table S3, Supporting Information): the C3d fragment, C3 complement, C3b complement and CLU.

Examples of the quantification of spots using DECODON software are shown in Figure 1B for C3 (Spot no.163; Table S2, Supporting Information) and two isoforms of RBP4 (Spot no.192 and 194; Table S2, Supporting Information). Interestingly, 66 out of the 126 regulated spots represented proteins that are related to pathways of apoptosis, classical, alternative or lectin pathways of complement activation (Figure 1C). These changes of set-related protein abundances between lean and obese meet the significance criterion for the pathway-related protein sets despite the relative large scattering of the individual data. In fact, no statistically relevant differences between lean and obese could be identified after applying the analogous analysis using disease-related protein sets (Figure S2, Supporting Information).

To extract the time effect, correlating with treatment, we performed ANOVA analysis separately for the data of both test groups: In the proteome study of fat mass independent protein changes in response to an acute exercise bout, 37 spots were found to vary significantly for obese and 39 for lean persons. Their assignment to different groups is displayed in the Volcano plots and Venn diagram (Figure 2B and C). The following seven proteins regulated in both groups were identified: C3, PEDF,

dx.doi.org/10.1021/pr2005555 |*J. Proteome Res.* 2011, 10, 4769–4788

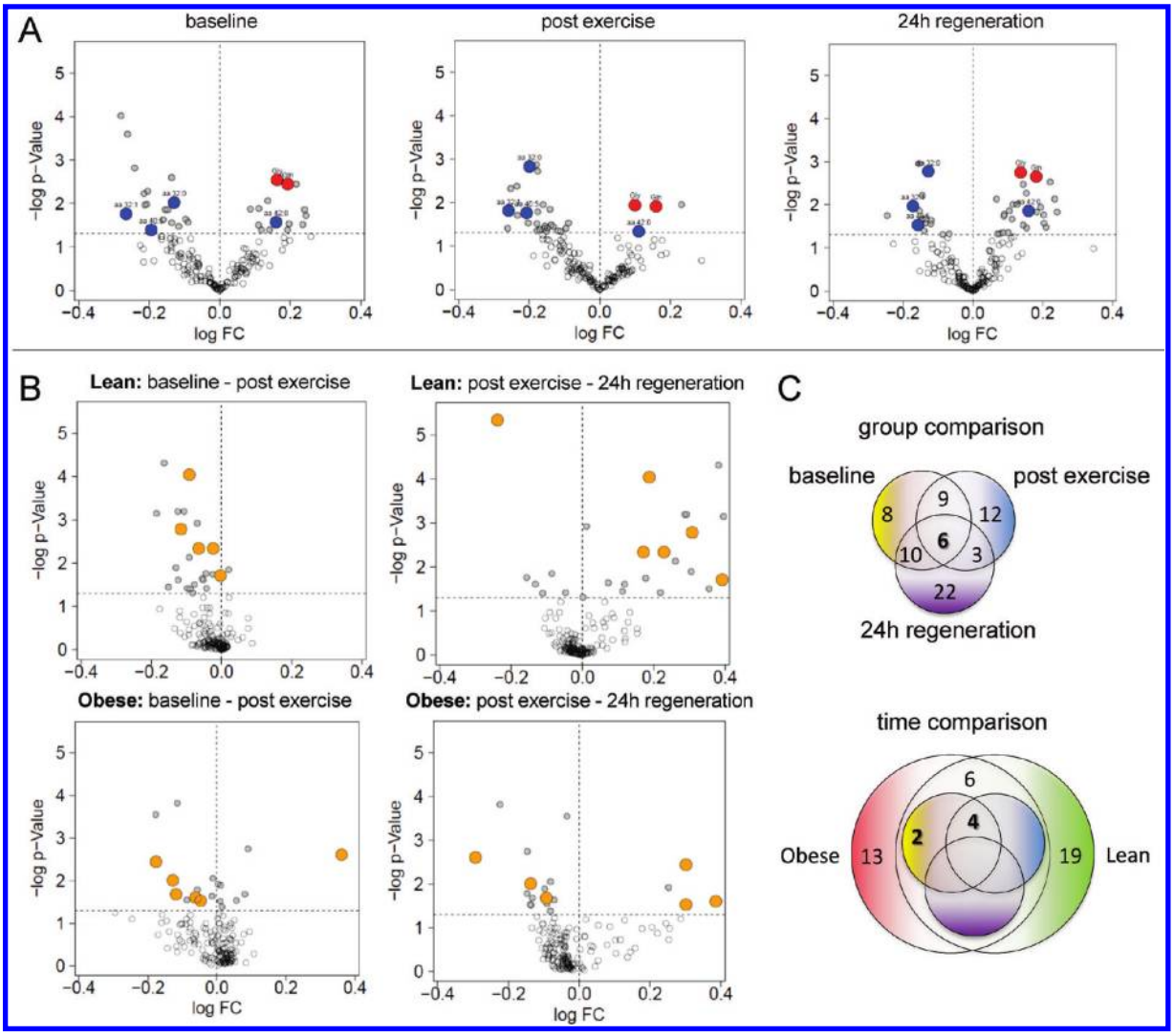

Figure 4. Metabolomic fingerprint from healthy lean and obese subjects. The relative changes in abundance of metabolites are shown as Vulcano plots for (A) group dependant comparisons and (B) over time. Minus log fold-change (FC) in A indicates up-regulation in obese subjects. The horizontal dotted line represents the significance threshold ($p < 0.05$) and the significantly regulated metabolites are highlighted in red (glycine and glutamine), blue (PCaa) and yellow (carnitines). The results are summarized as (C) Venn diagramm exhibiting the commonly and specifically affected metabolites.

SAP, RBP4, VDBP, AT III and KNG1 isoform 2 (Figure 3A, Tables S2, S3, Supporting Information). In spot no. 118 (for quantification see Figure 3A) AT III and KNG1 isoform 2 were found with similar scores (Table S2, Supporting Information). By means of specific ELISAs, we confirmed protein differences for C3 and CLU at all three points in time, for C3b, PEDF, RBP4, VDBP and AT III at two points and for SAP at a single point.

Identification of Six Metabolites As Exercise-Independent Predictors of Fat Mass Differences in Healthy Individuals

We investigated the metabolomic profiles of the same ten healthy lean and obese subjects at the three points in time with a prespecified particular focus on circulating amino acids, fatty acids, phospholipids and sphingolipids by targeted analysis of 163 metabolites[34] (Figure S1A, Supporting Information). Figure 4A shows results of paired *t* tests designed in correspondence with the analysis of proteome data. The abundance of six metabolites significantly differs between lean and obese volunteer's at all three points. Particularly, GLY, GLN and glycero-phosphatidylcholine 42:0 (PCaa 42:0) were up-regulated whereas glycero-phosphatidylcholine 32:0 (PCaa 32:0), glycero-phosphatidylcholine 32:1 (PCaa 32:1) and glycero-phosphatidylcholine 40:5 (PCaa 40:5) were down-regulated in obese volunteers (Table S4, Supporting Information). We identified 13 metabolites in the obese and 19 in the lean group, which were significantly and independently of fat mass differences altered in response to the exercise bout. Among them, six metabolites were commonly affected in both groups, that is, the carnitines C2, C10:1, C14:1-OH, C14:2, C18:1 and C18:2 n (Figure 4; Table S4, Supporting Information). The values for the enlarged cohort confirm these results on a broader basis (see Table S6, Supporting Information).

Combined Analysis of Proteome and Metabolome Data Sets Markedly Improves Discrimination between Lean and Obese Individuals

Proteome and metabolome data were either separately or combined subjected to ICA analysis in order to test if regulated proteins or metabolites or the combination of both data sets allow a better discrimination between obese and lean individuals

dx.doi.org/10.1021/pr2005555 |*J. Proteome Res.* 2011, 10, 4769–4788

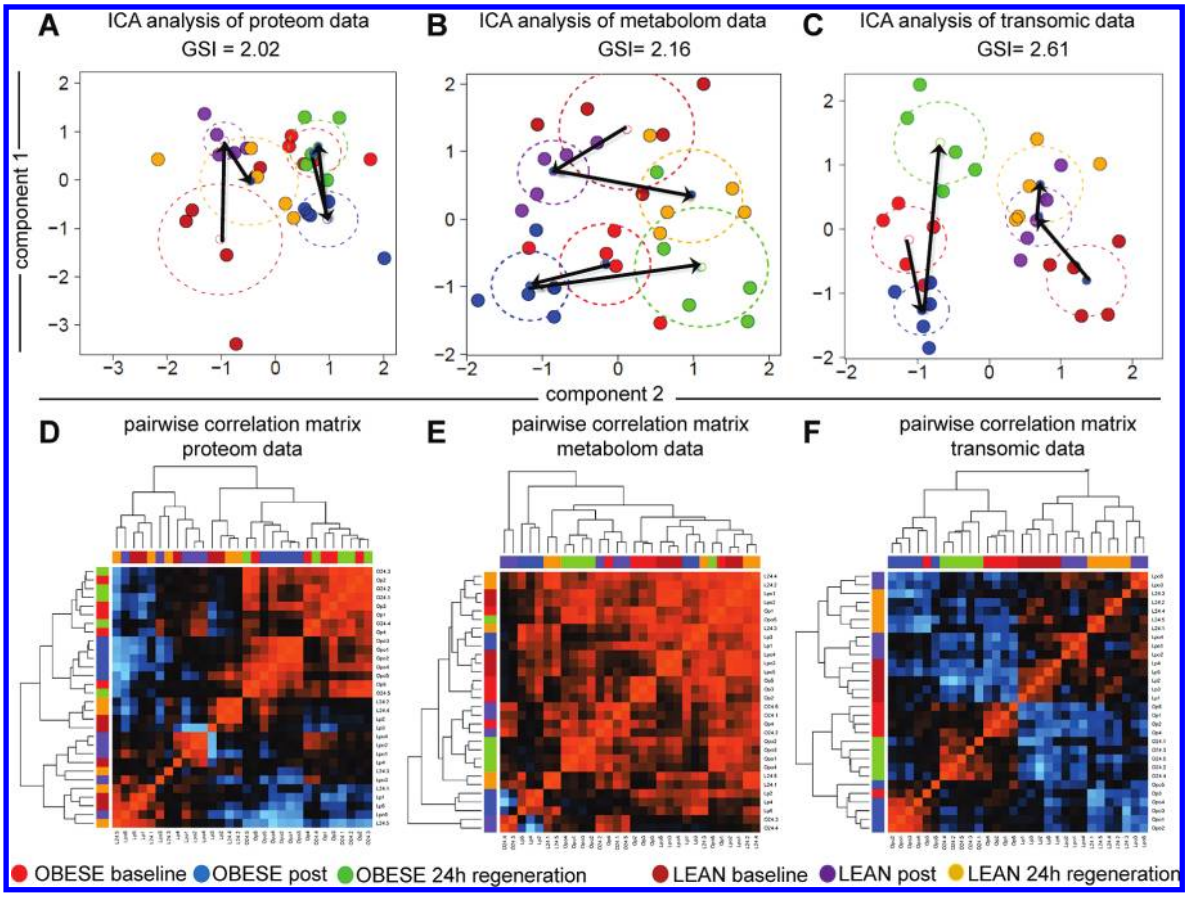

Figure 5. ICA analysis of single and of integrated data sets by ICA. ICA of (A) proteome and (B) metabolome data results in modest group separation which is improved by (C) analysis of an integrated data set. The dashed circles illustrate the variability of the five replicates measured at each condition. The group separation index (GSI) is calculated as the mean distance between the samples of different groups divided by the mean distance between the samples of the same group. The arrows illustrate the sequence of time points.

and/or between the exercising conditions (Figure 5). ICA aggregates the set of proteins and/or metabolites studied into one point per sample in the two-dimensional coordinate system spanned by the two most relevant independent components (Figure 5). The mean position characterizing each condition was calculated as the center of gravity of the respective replicated samples (small open circles). The dashed circle drawn about each center of gravity illustrates the mean Euclidian distance between the replicates as a measure of their variability.

The ICA-plots thus show one cloud of replicated samples with different mutual distances between their centers of gravity referring either to the different points in time or volunteer groups. The sequence of points in response to an exercise bout is indicated by the arrows separately for obese and lean volunteers (Figure 5A−C). These trajectories reveal that both the proteome and metabolome profiles markedly change immediately after exercising. Upon regeneration, the profiles returns toward the baseline situation partly with the tendency of overcompensation. Note also that these treatment-induced trajectories of both groups are roughly directed in parallel but shifted to each other in perpendicular directions. In ICA-coordinates, this fact indicates that the differential features between both groups are mostly independent of the differential features describing the treatment.

The mutual separations between the centroids are different for the proteomic, metabolomic and combined data sets. They were estimated in terms of the group separation index (GSI), which is defined as the mean distance between the different centroids divided by the mean distance between the replicates about the centroids. Hence, the larger the GSI-value the better the different conditions are resolved in the ICA coordinate system. The separate consideration of proteome and metabolome data provides similar values of GSI = 2.02 and 2.16, respectively (Figure 5A, B) whereas the combined ICA-analysis of both data sets markedly improves the discrimination between the different conditions (GSI = 2.61). In addition, we estimated partial GSI values between selected subgroups to characterize their relative distance in the ICA plot as simple measures of their discrimination power. At all conditions, proteome data outperform metabolome data for group separation lean versus- obese (Figure S3A, Supporting Information), whereas the reverse relation was observed for the discrimination between the different points in time (Figure S3B, Supporting Information). On one hand, the former result can be partly attributed to the preselection of differently expressed proteins in our study while the set of metabolites contains more analytes not different between the groups. On the other hand, similar preselection of metabolite data does virtually not change the observed differences because the respective noise is largely filtered out by ICA-analysis (data not shown). Hence, the obtained combined transomics data set outperforms the single-omics data in terms of group separation (compare Figure 5C with 5A and B). Trivially, this gain of

Table 2. Clinical Characteristics of Study 2 Subjects[a]

	control (n = 17)	low-carbohydrate diet (n = 12)			bariatric surgery (n = 14)		
	baseline	baseline	6 month post	p-value	baseline	6 month post	p-value
Age [years]	49 (±11.4)	49 (±2.71)			41.9 (±13.29)		
Type 2 diabetes — no. [%]	0	0	0		8	0	
Height [cm]	167.8 (±8.61)	171 (±10.27)			173.6 (±9.328)		
BW [kg]	74.8 (±11.3)	107.0 (±16.23)[b]	101.3 (±14.32)[b]	<0.001	164.0 (±33.83)[b]	110.6 (±28.31)[b]	<0.001
BF[%]	32.5 (±8.4)	38.0 (±2.9)[b]	35.4 (±3.0)	<0.001	56.1 (±8.3)[b]	38.5 (±7.2)[b]	<0.001
BMI [kg/m^2]	26.48 (±2.7)	36.42 (±2.77)[b]	34.51 (±2.53)[b]	<0.001	54.00 (±8.05)[b]	36.31 (±7.25)[b]	<0.001
HbA1 c [%]	4.92 (±0.3)	5.67 (±0.1 4)[b]	5.44 (±0.12)[b]	0.002	6.57 (±0.85)[b]	5.76 (±0.35)[b]	<0.004
FPG[mmol/L]	5.21 (±0.6)	5.34 (±0.37)	5.36 (±0.26)	ns	6.07 (±0.63)[b]	5.66 (±0.28)[b]	<0.0122
FPI[pmol/L]	72.0 (±33.1)	122 (±28.1)[b]	89 (21.2)	0.008	382 (±1 64)[b]	182 (±72.4)[b]	<0.001
Triglycerides [mmol/L]	1.46 (±0.78)	1.71 (±0.16)	1.49 (±0.13)	0.0011	2.29 (±0.49)[b]	1.75 (±0.28)	<0.002
HDL-cholesterol [mmol/L]	1.40 (±0.28)	1.04 (±0.1 7)[b]	1.21 (±0.14)[b]	0.009	0.91 (±0.18)[b]	1.33 (±0.22)	<0.001
hsCRP[mg/L]	1.39 (±0.51)	2.11 (±0.76)[b]	1.60 (±0.60)	0.0019	4.36 (±1.43)[b]	1.50 (±0.68)	<0.001

[a] Data are presented as mean ± SD.; † indicate b [b] $p < 0.05$ using unpaired t-test statistics to compare control vs. treatment time point, p-value represent time effect within group.

performance at least partly results from the increased sample size of the combined data set. However, also the complementary sensitivity of the metabolome and proteome characteristics for short and long-term effects discussed above is expected to improve the discrimination power of the combined data owing to the explicit consideration of the covariance information between both data sets.

Concerted changes of metabolites and proteins are likely to be functionally associated with consequences for mutual correlations between both data sets. The PCM heat maps (Figure 5D−F) illustrate the degree of these correlations in all pairwise combinations of the samples. Panels D−F of the figure refer to the proteome, metabolome and to the integrated data set, respectively. Strong positive and negative correlations are coded in red and blue colors, respectively, while weak correlations are shown in black. Hierarchical clustering groups samples of similar correlations closely together forming red squared areas about the diagonal line in the PCM. As expected, proteome data distinguish well between the obese and lean groups (Figure 5D, the color bars at the edges of the maps code the different conditions), but with virtually poor separation between the different points in time of conditioning. Metabolome data show a tendency to cluster these time points together (Figure 5E). The integrated data clearly separate both experimental dimensions, namely long and short-term conditions (Figure 5F). In assessing the cluster structures, one has to take into account that the rotation of branches about their parent root does not change the information content. Detailed inspection of the heat map reveals that the obtained pattern is stabilized by positive and negative correlations that accumulate in diagonal and off-diagonal direction, respectively. Especially the latter type of correlations is much stronger expressed in the integrated data than in the single data. This result supports our hypothesis that cross-correlations between protein and metabolite concentrations improve the separation of different conditions in an orthogonal fashion.

Effect of Weight Reduction on Circulating Proteome and Metabolome Markers

To further investigate whether differences in serum proteome between lean and obese healthy individuals correlate with differences in body fat mass, we studied the effect of two weight loss strategies (diet and bariatric surgery) on anthropometric, clinical parameters (Table 2) as well as the differentially abundant proteins and metabolites. The protein levels of iC3b, CLU and ATIII were significantly reduced in the diet group, whereas more extensive weight loss in the bariatric surgery study caused significant changes in C3, CLU, PEDF, RBP4 and VDBP serum concentrations. The full set of proteomic and metabolomic parameters obtained in the intervention study is summarized in Table S7 (Supporting Information). Multivariate linear regression models were used to test whether changes in the serum parameters are independent of changes in BMI, % body fat and parameters of insulin sensitivity as well as glucose metabolism. Serum protein concentrations of CLU, PEDF, SAP, RBP4 and AT III significantly correlate with body fat mass even after adjusting to age, gender and HbA1c (Table S8A, Supporting Information). The corresponding metabolomics approach showed significant correlations with changes in % BF for GLN, Carnitine C14:1OH, C18:1, C18:2 and C2 (Table S8B, Supporting Information). In addition, GLN, PCaa40:5, Carnitine C10:1 and C14:1OH correlate significantly with HbA1c. In the intervention studies, changes of CLU, PEDF iC3b and the metabolites GLN and PC 42 show significant correlations with changes in body fat mass after adjustment to age, gender, HbA1c and FPI (Tables 3 and 4). Interestingly, the changes in concentration of VDBP were not correlated to body fat changes.

DISCUSSION

Obesity is associated with an increased risk for metabolic and cardiovascular (CV) diseases. Altered secretion of bioactive molecules from excessive and dysfunction adipose tissue of most patients with obesity may at least in part be affected by this relationship.[2] Many novel adipokines, which could link fat accumulation to metabolic and CV diseases, have been described in the past decade. However, we intended to identify further circulating factors by combining proteomic and metabolomic approaches. In an exploratory study we compared the circulating proteome and metabolome, of 5 lean to 5 obese healthy young male volunteers (Table S1, Supporting Information), to exclude potential influences of already existing obesity-related comorbidities. The identified markers were then further analyzed in a set of

Table 3. Multiple Regression Analyses of Differential Proteins after Adjustment for Age, Gender, and Changes of BF (Model 1) and Age, Gender, ΔHbA1c, ΔBF (% of total weight), and ΔFPI (Model 2)

	β (p)							
parameter	ΔCLU	ΔC3	ΔPEDF	ΔSAP	ΔVDBP	Δ RBP4	ΔiC3b	Δ AT III
				Model 1				
Age	−0.338 ($p < 0.431$)	−0.003 ($p < 0.742$)	0.014 ($p < 0.357$)	0.409 ($p < 0.524$)	0.127 ($p < 0.941$)	0.057 ($p < 0.748$)	−0.005 ($p < 0.062$)	−0.469 ($p < 0.365$)
gender	−10.424 ($p < 0.220$)	−0.207 ($p < 0.237$)	−2.449 ($p < 0.266$)	3.357 ($p < 0.789$)	30.224 ($p < 0.370$)	−3.934 ($p < 0.261$)	−0.029 ($p < 0.566$)	−11.605 ($p < 0.256$)
Δ%BF	2.097 ($p < 0.000$)	0.008 ($p < 0.392$)	0.548 ($p < 0.001$)	1.153 ($p < 0.106$)	1.323 ($p < 0.476$)	0.414 ($p < 0.039$)	−0.012 ($p < 0.000$)	−0.691 ($p < 0.222$)
				Model 2				
Age	−0.354 ($p < 0.464$)	−0.004 ($p < 0.672$)	0.038 ($p < 0.801$)	0.686 ($p < 0.297$)	−0.151 ($p < 0.934$)	0.1 ($p < 0.612$)	−0.007 ($p < 0.007$)	−0.568 ($p < 0.322$)
gender	−10.828 ($p < 0.237$)	−0.253 ($p < 0.170$)	−2.801 ($p < 0.327$)	−1.064 ($p < 0. 93$)	18.448 ($p < 0.589$)	−4.055 ($p < 0.277$)	−0.044 ($p < 0.349$)	−9.723 ($p < 0.364$)
ΔHbA1$_c$	0.326 ($p < 0.975$)	−0.004 ($p < 0.986$)	−1.99 ($p < 0.541$)	−23.196 ($p < 0.107$)	−2.564 ($p < 0.948$)	−2.718 ($p < 0.522$)	0.112 ($p < 0.048$)	8.723 ($p < 0.476$)
Δ%BF	2.015 ($p < 0.006$)	0.001 ($p < 0.988$)	0.546 ($p < 0.014$)	1.072 ($p < 0.235$)	−0.696 ($p < 0.779$)	0.475 ($p < 0.088$)	−0.018 ($p < 0.000$)	−0.622 ($p < 0.425$)
ΔFPI	0.009 ($p < 0.853$)	0.001 ($p < 0.284$)	009 ($p < 0.526$)	0.115 ($p < 0. 077$)	0.261 ($p < 0.147$)	0.005 ($p < 0.802$)	0.001 ($p < 0.321$)	−0.048 ($p < 0.383$)

15 lean vs 15 obese volunteers (Table 1). All protein markers found in the smaller group were confirmed analyzing a 3-fold larger group and using an independent method of quantification. This can be explained by the fact that DIGE detects the proteins of higher and intermediate abundance and by the applied stringent statistical filters. To minimize the risk of identifying proteins and metabolites that reflect differences in physical activity between the groups, we applied an acute exercise bout study as a filter for those circulating factors.

Our proteome analysis revealed a higher abundance of C3, C3b, PEDF, SAP, RBP4, VDBP and ATIII in healthy obese than in lean individuals. The application of 2D gel electrophoresis enabled us to further detect post-translational modifications of proteins including C3, C3b and RBP4. Targeted metabolite profiling identified the amino acid GLN, and the carnitines C14:1OH, C18:1, C18:2 and C2 as differentially abundant in the serum of the two groups. In fact, these parameters were different in lean and obese individuals independently of physical activity status. Opposing lean and obese subjects, a transomics approach of proteome and metabonome data set increases the discrimination power of the data between both the treatment groups and treatment conditions compared with "single-OME" sets of metabonomic or proteomic data using the GSI-score as a simple criterion based on ICA analysis. We confirmed the potential role of these circulating factors as biomarkers of fat mass or potential mediators of obesity-associated disorders by demonstrating that changes in fat mass in response to a diet or bariatric surgery are reflected by changes in CLU, PEDF, RBP4, iC3b, GLN and glycero-phosphatidylcholine PCaa 42:0.

Fat Mass-Related Proteome Biomarkers

Our analysis aimed at identifying proteomic biomarkers in early stages of obesity without comorbidities, first, related to fat mass itself and, second, related to changes of body fat mass. By means of 2D gel electrophoresis, we identified 6 isoforms of C3 complement to be up-regulated in serum of young males with obesity and confirmed these differences by ELISA (Figure 3). C3 was not influenced either by one hour exercise treatment or by 24 h of regeneration and consistently discriminates lean and obese subjects (Figure 3D). It has previously been shown that C3 is secreted by adipocytes[35,36] and that its fragment C3a-des-Arg, or acylation-stimulating protein,[37] is a potent enhancer of glucose transport and triacylglycerol synthesis.[38] After bariatric surgery and low-carbohydrate diet, C3 was down-regulated (Table S7, Supporting Information). Interestingly, correlation between circulating C3 and body fat mass was discarded after adjustment to age, gender and HbA1c (Tables S8A and 3, Supporting Information). In the past decade, it has been revealed that C3 is highly expressed in adipose tissue of obese individuals.[39,40] In addition, C3 was shown to predict the risk of atrial fibrillation[41] or coronary artery disease[42] better than CRP levels. Our results further suggest that complement C3 plays a role as an early marker for obesity-related cardiovascular diseases.

CLU is a nearly ubiquitously expressed ~80 kDa disulfide-linked heterodimeric protein. In serum, it acts as an apolipoprotein, which at least partly associates with high density lipoprotein.[43] CLU has been functionally implicated in several physiological processes as well as in many pathological conditions including aging, diabetes, atherosclerosis, degenerative diseases, and tumorigenesis. The spectrum of proposed functions of CLU includes lipoprotein transport, inhibition of complement-mediated lysis, regulation of sperm maturation, cell

Table 4. Multiple Regression Analyses of Differential Metabolites after Adjustment for Age, Gender, and Changes of BF (Model 1) and Age, gender, ΔHbA1 C, ΔBF (% of total weight) and ΔFPI (Model 2)

	β (p)										
parameter	GLN	GLY	PC C32:1	PC C40:5	PC C42:0	carnitine C10:1	carnitine C14:1OH	carnitine C14:2	carnitine C18:1	Ccarnitine C18:2	carnitine C2
						Model 1					
Age	−1.316	−4.659	0.105	−0.022	−0.002	0.002	0.001	0.001	−0.002	−0.001	0.059
	($p < 0.357$)	($p < 0.003$)	($p < 0.139$)	($p < 0.582$)	($p < 0.580$)	($p < 0.248$)	($p < 0.366$)	($p < 0.663$)	($p < 0.068$)	($p < 0.102$)	($p < 0.508$)
gender	−31.303	−13.650	−1.653	−0.696	0.099	−0.013	−0.001	0.005	−0.005	−0.003	−1.684
	($p < 0.266$)	($p < 0.616$)	($p < 0.231$)	($p < 0.383$)	($p < 0.132$)	($p < 0.647$)	($p < 0.584$)	($p < 0.445$)	($p < 0.787$)	($p < 0.653$)	($p < 0.335$)
Δ%BF	−5.318	1.120	0.011	−0.082	0.015	0.002	7.450×10^{-5}	0.001	0.001	0.001	−0.027
	($p < 0.002$)	($p < 0.458$)	($p < 0.881$)	($p < 0.072$)	($p < 0.000$)	($p < 0.305$)	($p < 0.574$)	($p < 0.739$)	($p < 0.433$)	($p < 0.025$)	($p < 0.777$)
						Model 2					
Age	−2.069	−3.56	0.029	−0.045	0.002	0.002	0.001	0.001	−0.002	−0.001	0.049
	($p < 0.1$ 87)	($p < 0.018$)	($p < 0.638$)	($p < 0.306$)	($p < 0.465$)	($p < 0.32$)	($p < 0.419$)	($P < 0.77$)	($p < 0.148$)	($p < 0.107$)	($p < 0.623$)
gender	−32.2	−8.659	−1.968	−0.625	0.112	−0.014	−0.001	−0.006	−0.01	−0.006	−1.847
	($p < 0.269$)	($p < 0.742$)	($p < 0.104$)	($p < 0.441$)	($p < 0.044$)	($p < 0.630$)	($p < 0.584$)	($p < 0.461$)	($p < 0.601$)	($p < 0.377$)	($p < 0.325$)
ΔHbA1$_c$	42.475	−56.072	3.911	1.416	−0.207	0.001	0.001	0.002	−0.025	−0.004	−0.315
	($p < 0.206$)	($p < 0.074$)	($p < 0.008$)	($p < 0.136$)	($p < 0.002$)	($p < 0.991$)	($p < 0.941$)	($p < 0.829$)	($p < 0.26$)	($p < 0.612$)	($p < 0.882$)
Δ%BF	−6.77	3.716	−0.164	−0.112	0.024	0.001	6.313×10^{-5}	0.001	0.001	0.001	−0.066
	($p < 0.004$)	($p < 0.064$)	($p < 0.066$)	($p < 0.068$)	($p < 0.000$)	($p < 0.559$)	($p < 0.737$)	($p < 0.686$)	($p < 0.618$)	($p < 0.323$)	($p < 0.629$)
ΔFPI	−0.013	−0.066	0.004	−0.003	0.001	3.675×10^{-5}	2.402×10^{-6}	3.075×10^{-6}	0.001	6.836×10^{-5}	0.003
	($p < 0.93$)	($p < 0.624$)	($p < 0.519$)	($p < 0.522$)	($p < 0.679$)	($p < 0.812$)	($p < 0.856$)	($p < 0.936$)	($p < 0.202$)	($p < 0.063$)	($p < 0.727$)

dx.doi.org/10.1021/pr2005555 |J. Proteome Res. 2011, 10, 4769–4788

migration, and apoptosis[44] as well as suppression of the growth of extracellular amyloid.[45] Our exercise bout study shows opposite expression pattern of CLU after one hour of exercise in lean and obese volunteers (Figure 3F). CLU gene expression was shown to be regulated by cytokines, growth factors, heat shock proteins, radiation and oxidative stress.[46] Since acute exercise may increase circulating reactive oxygen species (ROS)[47] and cytokines,[48] increased ROS production might underlie the observed exercise-dependent increase in serum CLU. Changes of CLU correlate with body fat mass independent of age, gender, HbA1c and fasting plasma insulin (Table 3).

PEDF is one of the most abundant proteins secreted by human adipocytes and induces insulin resistance in adipocytes and skeletal muscle cells.[49] Elevated PEDF plasma concentrations have been reported in patients with metabolic syndrome and type 2 diabetes, abdominal fat distribution and in individuals with high triglycerides, creatinine and TNF-alpha serum concentrations.[50−52] In our study, elevated levels of PEDF were already abundant in young obese subjects without clinical signs of altered glucose homeostasis and could be reduced by acute exercise (Figure 3G) and substantial weight loss following bariatric surgery (Table S7, Supporting Information). This suggests PEDF as an early marker of obesity-related metabolic comorbidities, also in accordance with a previous study showing decreased PEDF concentrations after significant weight loss.[53] Serum PEDF correlates with body fat mass even after adjustment to age, gender and HbA1c (Table S8, Supporting Information). In contrast to sleeve gastrectomy, low carbohydrate diet-associated weight loss was not sufficient to significantly decrease circulating PEDF levels (Table S7, Supporting Information). PEDF has been shown to contribute to insulin resistance in obesity.[54] Our data indicate that increasing fat mass may be the earliest underlying mechanism for the relationship between elevated PEDF levels and altered insulin sensitivity.

SAP activates the classical component pathway and was shown to be involved in inflammation.[55−57] In this study, we detected elevated levels of SAP in obese subjects independently of an acute exercise bout (Figure 3H). Hence, we confirm previous results of elevated SAP in obesity.[58] Comparing sleeve gastrectomy and low carbohydrate diet, the dynamic in SAP serum concentrations has a divergent pattern (Table S7, Supporting Information). Substantial weight loss after surgical obesity treatment was associated with significantly decreased circulating SAP levels, whereas increased SAP was observed in patients with moderate weight loss after 6 months hypocaloric diet. Circulating SAP correlates with age and % body fat, independently of age, gender and HbA1c (Table S8, Supporting Information). However, changes in fat mass after the two different weight loss strategies were not related to changes in SAP serum concentrations, finally implying that adipose tissue does not represent the major source of SAP. SAP has been suggested to bind to chromatin in apoptotic cells, thereby repressing formation of autoantibodies.[59] In the context of our study, elevated levels of SAP may indicate subclinical chronic inflammation already in healthy obese individuals.

The identification of elevated RBP4 serum concentrations in obese compared to lean men by the proteomics approach testifies that the method is able to detect previously reported markers of increased fat mass. RBP4 has gained a lot of attention after the initial notion that it is elevated in the serum of insulin-resistant humans and mice[60] and that increased RBP4 serum concentrations are associated with many components of the metabolic syndrome.[61] In patients with obesity and type 2 diabetes, RBP4 was shown to be predominantly secreted from visceral adipose tissue.[62] However, as of today, a causal link between elevated serum RBP4 and increased fat accumulation beyond simple association could not be established convincingly. Our gel-based approach showed expression of two different isoforms of RBP4 up-regulated in obesity (Figure 1A−B). Both isoforms increased significantly after a one-hour exercise bout in lean volunteers and decreased in obesity (Table S3, Supporting Information). Our data points toward a previously unrecognized role of RBP4 isoforms that should be further investigated in the context of obesity. RBP4 isoforms were not further investigated, but it should be kept in mind that isoforms can be important for the regulation of biological processes.[63,64] Using ELISA to confirm our 2D approach with independent methods, RBP4 is differentially expressed in sera of obese volunteers (Figure 3I). After a one-hour exercise workout, significant differences between lean and obese were investigated. Interestingly, after 24 h of regeneration, the differences between the two groups have finally been achieved (Figure 3I). Increased serum RBP4 levels have been reported in subjects with obesity, insulin resistance, low grade chronic inflammation and type 2 diabetes[61] and in other insulin-resistant states, such as nonalcoholic fatty liver disease.[65] These pathological processes are also related to inflammation,[66] as reported for acute exercise.[67] Our results indicate that the serum expression rate of RBP4 is influenced by acute changes in metabolism and after long-term changes of glucose homeostasis by sleeve gastrectomy (Table S7, Supporting Information). This argument is supported by the fact that sleeve gastrectomy has been shown to rapidly increase insulin sensitivity[68] and thereby indicate a correlation with loss of fat mass.[69] In contrast to further recent studies, we were not able to detect an effect of hypocaloric diet in order to decrease RBP4 serum levels.[68] However, we could confirm an independent significant correlation of circulating RBP4 with body fat mass as well as changes in body fat percentage (Table S8, Supporting Information). Supporting previous data, the association between RBP4 and reduced body fat after 6 months was stronger than its association with BMI.[70,71] Circulating RBP4 levels also correlate with ectopic fat accumulation in the liver, visceral fat and skeletal muscle.[72] One potential mechanism for reduced RBP4 levels after bariatric surgery could therefore be a reduction in these ectopic fat depots.

VDBP is the major serum transport protein for vitamin D sterols.[73] The protein has been reported to be associated with diabetes and hyperglycemia in PIMA Indians and other ethnical groups.[74,75] We found significantly higher VDBP serum concentrations independently of the physical activity status in obese than in lean subjects (Figure 3J). After sleeve gastrectomy, VDBP levels decreased significantly but did not normalize, whereas low calorie diet was not sufficient to alter circulating VDBP (Table S7, Supporting Information). Furthermore, VDBP serum concentrations do not correlate with body fat mass (Table S8, Supporting Information). VDBP is a carrier protein for vitamin D hormone and the affinity of VDBP for 1.25 (OH)2 vitamin D3, and 25-OH-vitamin D3 differs depending on the genotype.[76] Vitamin D plays a role in the pathogenesis of impaired glucose homeostasis and has been associated with both insulin sensitivity and beta-cell function among individuals at risk for type 2 diabetes.[77−79] Thus, it is tempting to speculate that VDBP affects glucose metabolism by modulating the action of metabolites of vitamin D. Winters et al. (2009) showed that VDBP is not an important determinant of circulating 25OHD in women and that

it is not affected by adiposity.[80] On the other hand, morbidly obese patients seeking bariatric surgery are often deficient in Vit D.[81] This fact can explain why VDBP only shows changes in sleeve gastrectomy patients (Table S7, Supporting Information). Furthermore, it is recognized that bariatric surgery causes a hypovitaminosis of vitamin D.[82] To sum up, these findings shed light on a putative role of vitamin D-binding protein, but further investigations are necessary.

AT III exerts its function by inhibiting thrombin and is therefore involved in the regulation of coagulation.[83] Hemostasis is disturbed in obesity-related disorders such as Type 2 Diabetes and, therefore, it is characterized as a hypercoagulable state.[84] This state could be caused by either an increase of pro-coagglutination factors or a deficiency of anticoagglutination factors. We found elevated levels of AT III in obese subjects (Figure 3C). AT III serum concentrations correlate with body fat mass and HbA1c independently of age and gender (Table S8, Supporting Information). However, changes in body fat mass upon the two intervention strategies were not associated with changes in AT III levels, suggesting that fat mass does not directly cause elevated circulating AT III.

Taken together, the candidate biomarkers C3b, CLU and VDBP need further replication studies to identify the impact on the pathomechanism of obesity related disorders.

Fat Mass-Related Metabolome Biomarkers

Here, we detected GLN, the most abundant amino acid in plasma and in skeletal muscle (Lacey and Wilmore, 1990), and GLY as the strongest differentially abundant metabolite discriminating obese from lean subjects (Table S4, Supporting Information). Glutamine has been reported to play a role in maintenance of skeletal muscle, immune system function as well as glucose and glycogen metabolism.[85] Obese subjects exhibited significantly lower levels of glutamine at baseline and over the time course of physical activity and regeneration (Table S4, Supporting Information), finally indicating a robust association of this amino acid with obesity. Lower GLY serum concentrations can be increased by bariatric surgery (Table S7, Supporting Information), indicating that the increased fat mass contributes to lower circulating GLY. It could be further explained by the predominance of catabolic metabolism in which muscle tissue might secrete glutamine to enable maintaining glucose homeostasis by the liver. GLY is involved in many different biochemical mechanisms including the regulation of plasma cholesterol and triglyceride levels[86] as well as protection against D-galactosamine hepatotoxicity.[87] In earlier studies, GLY was shown to be useful in relation to diseases with an inflammatory component including the metabolic syndrome.[88] Recent results obtained in a mouse model of obesity show that GLY led to a suppression of pro-inflammatory cytokines such as TNF-alpha in adipose tissue and IL-6 serum levels and increased serum levels of adiponectin.[89] GLY was also found as an early marker for insulin resistance[20] but surprisingly was not found to be differentiating between lean and diabetic patients in another study,[21] pointing to an uncertain relation to the etiology of metabolic syndrome related disorders. In this study, neither low carbohydrate diet nor sleeve gastrectomy did affect GLY levels (Table S7, Supporting Information). Additionally, GLY showed neither a correlation to nor changes of fat mass (Table S8, Supporting Information). We hypothesize that decreased serum concentrations of GLY found in young obese are obviously related to nutritional status rather than to obesity itself.

GLN correlates with body fat mass and HbA1c value (Table S8, Supporting Information). Changes in GLN levels significantly correlate with changes of % body fat after weight reduction strategies independently of age, gender, fasting plasma insulin and HbA1c (Table 4). Since an effect of orally administered glutamine on serum concentration of glucagon-like peptide 1, glucose-dependent insulinotropic polypeptide (GIP) and glucagon was found,[90] it seems to be important to maintain a stable glutamine level. Among all measured metabolites GLN showed the strongest correlation to body fat and changes of fat mass (Table 4 and Table S8, Supporting Information). In other metabolome-wide studies, glutamine was not found as markers of insulin resistance in nondiabetic patients[20] neither as differential between lean and diabetes patients as a single marker,[21] but in relation to phenylacetylglutamine, it shows a significant correlation in the latter study.

Phosphatidylcholines are involved in lipid metabolism and are crucial for lipid transport. Concentrations of phosphatidylcholines have been related to the accumulation of fat in the liver.[91] Moreover, we found significantly higher abundance of the phosphatidylcholines PC32:0, PC32:1 and PC40:5 in obese compared to lean subjects (Table S6, Supporting Information). Although no phosphatidylcholine correlated with body fat mass at baseline, there was a significant correlation between changes in PC42:0 serum concentration and changes of body fat mass after both bariatric surgery and diet interventions (Table S8, Supporting Information).

Carnitines are essential for the transport of fatty acids into the mitochondria. In serum, C2 is the dominant carnitine species, which corresponds with the intracellular abundance of this carnitine. We found C2 highly elevated in obese subjects and immediately after exercise with a sustained elevation even 24 h after the acute exercise bout (Table S4, Supporting Information). Increased serum levels in obese subjects could be caused by mitochondrial damage occurring in skeletal muscle of obese patients.[92] After long-term metabolic changes by either hypocaloric diet or sleeve gastrectomy the levels did not change significantly but stayed stably compared to controls (Table S7, Supporting Information). As an exception, C14:1OH carnitine was correlated with body fat mass even after adjustment to age, gender and HbA1c (Table S8, Supporting Information). Our results indicate that carnitines in general are more related to acute changes of metabolism than to reflect long-term changes of fat mass. Also, carnitines may act as anti-inflammatory factors.[93] After physical exercise, carnitines were found to be affected over time using ANOVA (Table S4, Supporting Information). The majority of carnitines showed a general increase in lean and obese subjects under exercise-induced metabolism and recovery. In contrast, C2 was increased by exercise and decreased after 24 h of regeneration albeit C2 concentration did not reach the baseline level (Table S4, Supporting Information). This qualifies C2 as a potential indicator for differential states of metabolic activity between lean and obese subjects. Carnitines are relevant markers of mitochondrial efficiency: an increased level especially of short and intermediate carnitine indicate an impaired mitochondrial metabolism used for newborn screening.[94] In contrast to this study, various carnitines were found to be significant differentially abundant in plasma samples of obese and lean persons in a recent study.[95] Kim et al. discussed the elevated levels in obese patients by the positive effects of byproducts or intermediates of the branched chain amino acid catabolism. Additionally, It is well-known that inefficient tissue long-chain fatty

acid β-oxidation, due in part to a relatively low tricarboxylic acid cycle capacity, increases tissue accumulation of acetyl-CoA and generates chain-shortened acylcarnitine molecules. Comprehensive plasma acylcarnitine profiles in T2DM have revealed elevated circulating markers of incomplete LCFA catabolism and of acetylcarnitine.[96] Our work provides evidence that obese patients without comorbidities show different serum acylcarnitine profile both under exercise conditions and in relation to weight loss compared to lean subjects. This serum acylcarnitine profile appears to be a sensitive indicator of biochemical pathways that are responsive to the severity of diabetes and long-term blood sugar control.[96]

Combination of Proteomics and Metabolomics Improves Discrimination between Lean and Obese Subjects

Recent analyses demonstrated the potential of integrated "transomic" approaches.[32,97−99] However, so far only few examples exploit combinations of metabolomics and proteomics data.

We found that a combined proteome/metabolome approach allows a better group separation compared to the "single-OME" analyses (Figure 5A−C). An improved discrimination was also demonstrated for the exercise bout intervention. The better groupdiscrimination could be attributed to the increased sample size, but also to complementary sensitivities of the metabolites and proteins: Metabolites more strongly respond to short-term changes, whereas circulating proteins better reflect long-term adaptations. The combined analysis processes the covariances between protein and metabolite abundances that are not considered in the "single-omics" analysis. Such, correlations between both "omics" data obviously further improve the performance of the combined data. The additional benefit of these cross-correlations was supported by PCM analysis (Figure 5D−F) showing that the integrated data set separates the obese from the lean group very well, whereas "single-omics" data do not. These findings are in line with the results of studies on molecular plant physiology that also combine proteome and metabolome data sets.[32] Our results suggest that combination with selected proteomic markers such as proteins specifically expressed in adipose tissue might complement sets of metabolic risk markers.

In the past decade, technological developments provided broader studies on the metabolome of body fluids and cellular samples. Still, there are wide gaps in the information chain reaching from genes over proteins to metabolites. Even in relatively simple organisms such as the bacterium *Mycoplasma pneumonia* not all relevant genes and proteins for a validated metabolomic function could be detected by a recent large systems biology-oriented approach.[100] Nevertheless, all relevant levels of regulation must be combined in order to gain insights into factors governing physiological functions. The transomic approach applied in this study allowed us to detect parameters that are related to obesity independently of short-term exercise effects. However, the origin of the detected metabolites and proteins and their changes are not easy to define. By using clinically relevant interventions to reduce fat mass, we tested the hypothesis that adipose tissue is a major determinant of the production of differentially expressed parameters.

Pathways Related to Pathophysiology of Obesity

We hypothesized that our proteomic approach provides insights into pathway related changes that have already been detected in obese subjects in the absence of any obesity-related comorbidity. Our "shotgun-2D approach" allowed the quantitative determination of pathophysiological pathways such as apoptosis and complement system (Figure 1C). We found a "down-regulation of apoptosis" as one of the most prominent pathways associated with up-regulated protein abundances in obesity. Down-regulation of apoptosis could be an early indicator of obesity-related complications such as inflammation and increased oxidative stress. Additionally, proteins associated with three pathways of the complement system, namely the classical, the alternative and the MBL-pathway, are markedly increased in obese subjects (Figure 1C). The detection of the pathways of the complement system has strongly been influenced by the abundance of different isoforms of C3. Moreover, C3 is known to contribute to the formation of acylation stimulating protein whose level increases in obese people.[101] Decreased fat mass after hypocaloric diet or sleeve gastrectomy correlates with an increased activity of the complement system (Figure S4, Supporting Information). To our knowledge, this is the first study that showed correlations between the loss of fat mass and increased activity of the complement system.

Challenges in Proteomic and Metabolomic Profiling of Serum Samples

The two most prominent challenges in serum proteome analytics are the wide range of protein concentrations requiring depletion of high abundant proteins and their speciation owing to post-translational modifications.[12] For the latter purpose, 2D gels are still valuable tools, but for their application to serum samples, the high abundant proteins have to be depleted to obtain a wider coverage of the serum proteome. Classical 2D-gel electrophoresis leads to identification of selected spots but here we were interested in displaying dysregulation of homeostasis and the involved pathways.

Therefore the identification of 126 spots allowed for the analysis of pathways in a quantitative manner. Incomplete protein separation represents one well-recognized challenge in 2D gels leading to more than one protein per spot.[102] For example, spot 118 contains both AT III and KNG-1 with similar scores and had been unambiguously identified by nano-LC−MS/MS (Orbitrap-MS) (Table S2, Supporting Information). The relative contribution of both proteins to the spot intensity was analyzed by specific ELISAs revealing a stronger impact of AT III (Figure 3B,C). This example illustrates the limits of 2D-gel electrophoresis. Beyond the potential insights of the DIGE approach, it can represent only a fraction of the serum proteome. It is far from a comprehensive analysis but allows for detection of robust differences between diverse conditions. The serum metabolome displays some specific challenges like a wide range of concentrations of metabolites and its various origins.

In conclusion, integrated serum proteomic and metabolomic profiling reveals association of the complement system with obesity and identifies both novel and previously discovered markers of body fat mass changes. Multivariate regression analyses identified SAP, CLU, RBP4, PEDF, GLN and C18:2 as the strongest predictors of changes in body fat mass (Tables 3 and 4). Despite the validation in the two differently treated groups, there is still a demand to confirm the correlation of the so far potential markers to the change in body fat mass in larger and prospective cohorts.

■ ASSOCIATED CONTENT

Supporting Information

Supplemental tables and figures. This material is available free of charge via the Internet at http://pubs.acs.org.

AUTHOR INFORMATION

Corresponding Author

* Martin von Bergen. Address: Helmholtz Centre for Environmental Research, Department of Metabolomics, Permoser Strasse 15, 04318 Leipzig. Telephone: ++49-341-2351211. E-mail: Martin.vonbergen@ufz.de. Fax:++49-341-235451211.

ACKNOWLEDGMENT

This work was supported by the Competence network for Obesity funded by the Federal Ministry of Education and Research (FKZ 01GI0829), and a grant from Deutsche Forschungsgemeinschaft (DFG) to the Clinical Research group "Atherobesity" KFO 152/2 (project BL 833/1-1 to M.B.).

ABBREVIATIONS:

AT III, antithrombin-III; BF, body fat; BMI, body-mass index; BW, body weight; CLU, clusterin; C3b, complement C3b; iC3b, inactive complement C3b; GLN, glutamine; GLY, glycine; HDL, high density lipoprotein; KNG1, kinogen-1 isoform2; MS, mass spectrometry; PC, phosphatidylcholine; PEDF, pigment epithelium derived factor; RBP4, retinol binding protein; SAP, serum amyloid P; C3, serum complement C3; APOH, apolipoprotein H; HSA, human serum albumin; TG, triglyceride; VDBP, vitamin-D binding protein; FPI, fasting plasma insulin; FPG, fasting plasma glucose; OGTT, oral glucose tolerance test; BF, body fat; hSkMC, human skeletal muscle cells; hSMC, human smooth muscle cells

REFERENCES

(1) James, P. T.; Rigby, N.; Leach, R. The obesity epidemic, metabolic syndrome and future prevention strategies. *Eur. J. Cardiovasc. Prev. Rehabil.* **2004**, *11* (1), 3–8.

(2) Van Gaal, L. F.; Mertens, I. L.; De Block, C. E. Mechanisms linking obesity with cardiovascular disease. *Nature* **2006**, *444* (7121), 875–80.

(3) Guilherme, A.; Virbasius, J. V.; Puri, V.; Czech, M. P. Adipocyte dysfunctions linking obesity to insulin resistance and type 2 diabetes. *Nat. Rev. Mol. Cell Biol.* **2008**, *9* (5), 367–77.

(4) Bluher, M. Adipose tissue dysfunction in obesity. *Exp. Clin. Endocrinol. Diabetes* **2009**, *117* (6), 241–50.

(5) Sundsten, T.; Ortsater, H. Proteomics in diabetes research. *Mol. Cell. Endocrinol.* **2009**, *297* (1−2), 93–103.

(6) Griffin, J. L.; Nicholls, A. W. Metabolomics as a functional genomic tool for understanding lipid dysfunction in diabetes, obesity and related disorders. *Pharmacogenomics* **2006**, *7* (7), 1095–107.

(7) Mayr, M.; Mayr, U.; Chung, Y. L.; Yin, X.; Griffiths, J. R.; Xu, Q. Vascular proteomics: linking proteomic and metabolomic changes. *Proteomics* **2004**, *4* (12), 3751–61.

(8) Schiess, R.; Wollscheid, B.; Aebersold, R. Targeted proteomic strategy for clinical biomarker discovery. *Mol. Oncol.* **2009**, *3* (1), 33–44.

(9) Liu, B.; Qiu, F.; Voss, C.; Xu, Y.; Zhao, M. Z.; Wu, Y. X.; Nie, J.; Wang, Z. L. Evaluation of three high abundance protein depletion kits for umbilical cord serum proteomics. *Proteome Sci.* **2011**, *9* (1), 24.

(10) Linke, T.; Doraiswamy, S.; Harrison, E. H. Rat plasma proteomics: effects of abundant protein depletion on proteomic analysis *J. Chromatogr., B: Anal. Technol. Biomed. Life Sci.* **2007**, *849* (1−2), 273–81.

(11) Cellar, N. A.; Karnoup, A. S.; Albers, D. R.; Langhorst, M. L.; Young, S. A. Immunodepletion of high abundance proteins coupled online with reversed-phase liquid chromatography: a two-dimensional LC sample enrichment and fractionation technique for mammalian proteomics. *J. Chromatogr., B: Anal. Technol. Biomed. Life Sci.* **2009**, *877* (1−2), 79–85.

(12) Jungblut, P. R.; Holzhutter, H. G.; Apweiler, R.; Schluter, H. The speciation of the proteome. *Chem. Cent. J.* **2008**, *2*, 16.

(13) Unlu, M.; Morgan, M. E.; Minden, J. S. Difference gel electrophoresis: a single gel method for detecting changes in protein extracts. *Electrophoresis* **1997**, *18* (11), 2071–7.

(14) Altmaier, E.; Kastenmuller, G.; Romisch-Margl, W.; Thorand, B.; Weinberger, K. M.; Adamski, J.; Illig, T.; Doring, A.; Suhre, K. Variation in the human lipidome associated with coffee consumption as revealed by quantitative targeted metabolomics. *Mol. Nutr. Food Res.* **2009**, *53* (11), 1357–65.

(15) Gieger, C.; Geistlinger, L.; Altmaier, E.; Hrabe de Angelis, M.; Kronenberg, F.; Meitinger, T.; Mewes, H. W.; Wichmann, H. E.; Weinberger, K. M.; Adamski, J.; Illig, T.; Suhre, K. Genetics meets metabolomics: a genome-wide association study of metabolite profiles in human serum. *PLoS Genet.* **2008**, *4* (11), e1000282.

(16) Griffiths, W. J.; Koal, T.; Wang, Y.; Kohl, M.; Enot, D. P.; Deigner, H. P., Targeted Metabolomics for Biomarker Discovery. *Angew. Chem., Int. Ed. Engl.* **2010**, *49* (32), 5426−45.

(17) Jonsson, B. A.; Richthoff, J.; Rylander, L.; Giwercman, A.; Hagmar, L. Urinary phthalate metabolites and biomarkers of reproductive function in young men. *Epidemiology* **2005**, *16* (4), 487–93.

(18) Stahlhut, R. W.; van Wijngaarden, E.; Dye, T. D.; Cook, S.; Swan, S. H. Concentrations of urinary phthalate metabolites are associated with increased waist circumference and insulin resistance in adult U.S. males. *Environ. Health Perspect.* **2007**, *115* (6), 876–82.

(19) Oberbach, A.; von Bergen, M.; Till, H., Combined serum proteomic and metabonomic profiling following laparoscopic sleeve gastrectomy in children and adolescents. *Journal of Laparoendoscopic & Advanced Surgical Techniques* **2011**, *21* (4), A-1-A-92. doi:10.1089/lap.2011.9999.

(20) Gall, W. E.; Beebe, K.; Lawton, K. A.; Adam, K. P.; Mitchell, M. W.; Nakhle, P. J.; Ryals, J. A.; Milburn, M. V.; Nannipieri, M.; Camastra, S.; Natali, A.; Ferrannini, E. Alpha-hydroxybutyrate is an early biomarker of insulin resistance and glucose intolerance in a nondiabetic population. *PLoS One* **2010**, *5* (5), e10883.

(21) Suhre, K.; Meisinger, C.; Doring, A.; Altmaier, E.; Belcredi, P.; Gieger, C.; Chang, D.; Milburn, M. V.; Gall, W. E.; Weinberger, K. M.; Mewes, H. W.; Hrabe de Angelis, M.; Wichmann, H. E.; Kronenberg, F.; Adamski, J.; Illig, T. Metabolic footprint of diabetes: a multiplatform metabolomics study in an epidemiological setting. *PLoS One* **2010**, *5* (11), e13953.

(22) Seelen, M. A.; Roos, A.; Wieslander, J.; Mollnes, T. E.; Sjoholm, A. G.; Wurzner, R.; Loos, M.; Tedesco, F.; Sim, R. B.; Garred, P.; Alexopoulos, E.; Turner, M. W.; Daha, M. R. Functional analysis of the classical, alternative, and MBL pathways of the complement system: standardization and validation of a simple ELISA. *J. Immunol. Methods* **2005**, *296* (1−2), 187–98.

(23) Morbt, N.; Tomm, J.; Feltens, R.; Mogel, I.; Kalkhof, S.; Murugesan, K.; Wirth, H.; Vogt, C.; Binder, H.; Lehmann, I.; von Bergen, M. Chlorinated benzenes cause concomitantly oxidative stress and induction of apoptotic markers in lung epithelial cells (A549) at nonacute toxic concentrations. *J. Proteome Res.* **2011**, *10* (2), 363–78.

(24) Santos, P. M.; Roma, V.; Benndorf, D.; von Bergen, M.; Harms, H.; Sa-Correia, I. Mechanistic insights into the global response to phenol in the phenol-biodegrading strain Pseudomonas sp. M1 revealed by quantitative proteomics. *OMICS* **2007**, *11* (3), 233–51.

(25) Jehmlich, N.; Schmidt, F.; Taubert, M.; Seifert, J.; von Bergen, M.; Richnow, H. H.; Vogt, C. Comparison of methods for simultaneous identification of bacterial species and determination of metabolic activity by protein-based stable isotope probing (Protein-SIP) experiments. *Rapid Commun. Mass Spectrom.* **2009**, *23* (12), 1871–8.

(26) Jehmlich, N.; Schmidt, F.; Hartwich, M.; von Bergen, M.; Richnow, H. H.; Vogt, C. Incorporation of carbon and nitrogen atoms into proteins measured by protein-based stable isotope probing (Protein-SIP). *Rapid Commun. Mass Spectrom.* **2008**, *22* (18), 2889–97.

(27) Muller, S. A.; Kohajda, T.; Findeiss, S.; Stadler, P. F.; Washietl, S.; Kellis, M.; von Bergen, M.; Kalkhof, S., Optimization of parameters for coverage of low molecular weight proteins. *Anal. Bioanal. Chem.* **2010**, *398* (7−8), 2867−81.

(28) Strimmer, K. A unified approach to false discovery rate estimation. *BMC Bioinform.* **2008**, *9*, 303.
(29) Cui, X.; Churchill, G. A. Statistical tests for differential expression in cDNA microarray experiments. *Genome Biol.* **2003**, *4* (4), 210.
(30) Henegar, C.; Tordjman, J.; Achard, V.; Lacasa, D.; Cremer, I.; Guerre-Millo, M.; Poitou, C.; Basdevant, A.; Stich, V.; Viguerie, N.; Langin, D.; Bedossa, P.; Zucker, J. D.; Clement, K. Adipose tissue transcriptomic signature highlights the pathological relevance of extracellular matrix in human obesity. *Genome Biol.* **2008**, *9* (1), R14.
(31) Hyvarinen, A.; Oja, E. Independent component analysis: algorithms and applications. *Neural Netw.* **2000**, *13* (4−5), 411–30.
(32) Morgenthal, K.; Wienkoop, S.; Wolschin, F.; Weckwerth, W. Integrative profiling of metabolites and proteins: improving pattern recognition and biomarker selection for systems level approaches. *Methods Mol. Biol.* **2007**, *358*, 57–75.
(33) Ackermann, M.; Strimmer, K. A general modular framework for gene set enrichment analysis. *BMC Bioinform.* **2009**, *10*, 47.
(34) Koal, T.; Deigner, H. P. Challenges in mass spectrometry based targeted metabolomics. *Curr. Mol. Med.* **2010**, *10* (2), 216–26 .
(35) Zimmer, B.; Hartung, H. P.; Scharfenberger, G.; Bitter-Suermann, D.; Hadding, U. Quantitative studies of the secretion of complement component C3 by resident, elicited and activated macrophages. Comparison with C2, C4 and lysosomal enzyme release. *Eur. J. Immunol.* **1982**, *12* (5), 426–30.
(36) Alvarez-Llamas, G.; Szalowska, E.; de Vries, M. P.; Weening, D.; Landman, K.; Hoek, A.; Wolffenbuttel, B. H.; Roelofsen, H.; Vonk, R. J. Characterization of the human visceral adipose tissue secretome. *Mol. Cell. Proteomics* **2007**, *6* (4), 589–600.
(37) Germinario, R.; Sniderman, A. D.; Manuel, S.; Lefebvre, S. P.; Baldo, A.; Cianflone, K. Coordinate regulation of triacylglycerol synthesis and glucose transport by acylation-stimulating protein. *Metabolism* **1993**, *42* (5), 574–80.
(38) Baldo, A.; Sniderman, A. D.; St-Luce, S.; Avramoglu, R. K.; Maslowska, M.; Hoang, B.; Monge, J. C.; Bell, A.; Mulay, S.; Cianflone, K. The adipsin-acylation stimulating protein system and regulation of intracellular triglyceride synthesis. *J. Clin. Invest.* **1993**, *92* (3), 1543–7.
(39) Gabrielsson, B. G.; Johansson, J. M.; Lonn, M.; Jernas, M.; Olbers, T.; Peltonen, M.; Larsson, I.; Lonn, L.; Sjostrom, L.; Carlsson, B.; Carlsson, L. M. High expression of complement components in omental adipose tissue in obese men. *Obes. Res.* **2003**, *11* (6), 699–708.
(40) Peake, P. W.; Kriketos, A. D.; Campbell, L. V.; Charlesworth, J. A. Response of the alternative complement pathway to an oral fat load in first-degree relatives of subjects with type II diabetes. *Int. J. Obes. (London)* **2005**, *29* (4), 429–35.
(41) Dernellis, J.; Panaretou, M. Effects of C-reactive protein and the third and fourth components of complement (C3 and C4) on incidence of atrial fibrillation. *Am. J. Cardiol.* **2006**, *97* (2), 245–8.
(42) Ajjan, R.; Grant, P. J.; Futers, T. S.; Brown, J. M.; Cymbalista, C. M.; Boothby, M.; Carter, A. M. Complement C3 and C-reactive protein levels in patients with stable coronary artery disease. *Thromb. Haemost.* **2005**, *94* (5), 1048–53.
(43) Jenne, D. E.; Lowin, B.; Peitsch, M. C.; Bottcher, A.; Schmitz, G.; Tschopp, J. Clusterin (complement lysis inhibitor) forms a high density lipoprotein complex with apolipoprotein A-I in human plasma. *J. Biol. Chem.* **1991**, *266* (17), 11030–6.
(44) Trougakos, I. P.; Gonos, E. S. Clusterin/apolipoprotein J in human aging and cancer. *Int. J. Biochem. Cell Biol.* **2002**, *34* (11), 1430–48.
(45) Hatters, D. M.; Wilson, M. R.; Easterbrook-Smith, S. B.; Howlett, G. J. Suppression of apolipoprotein C-II amyloid formation by the extracellular chaperone, clusterin. *Eur. J. Biochem.* **2002**, *269* (11), 2789–94.
(46) Trougakos, I. P.; Gonos, E. S. Chapter 9: Oxidative stress in malignant progression: The role of Clusterin, a sensitive cellular biosensor of free radicals. *Adv. Cancer Res.* **2009**, *104*, 171–210.
(47) Cakir-Atabek, H.; Demir, S.; PinarbaSili, R. D.; Gunduz, N. Effects of different resistance training intensity on indices of oxidative stress. *J. Strength Cond. Res.* **2010**, *24* (9), 2491–7 .
(48) Calle, M. C.; Fernandez, M. L. Effects of resistance training on the inflammatory response. *Nutr. Res. Pract.* **2010**, *4* (4), 259–69.
(49) Famulla, S.; Lamers, D.; Hartwig, S.; Passlack, W.; Horrighs, A.; Cramer, A.; Lehr, S.; Sell, H.; Eckel, J. Pigment epithelium-derived factor is one of the most abundant proteins secreted by human adipocytes and induces insulin resistance and inflammatory signaling in muscle and fat cells. *Int. J. Obes. (London)* **2011**, *35* (6), 762–72.
(50) Nakamura, K.; Yamagishi, S.; Adachi, H.; Kurita-Nakamura, Y.; Matsui, T.; Inoue, H. Serum levels of pigment epithelium-derived factor (PEDF) are positively associated with visceral adiposity in Japanese patients with type 2 diabetes. *Diabetes Metab. Res. Rev.* **2009**, *25* (1), 52–6.
(51) Matsuyama, K.; Ogata, N.; Matsuoka, M.; Shima, C.; Wada, M.; Jo, N.; Matsumura, M. Relationship between pigment epithelium-derived factor (PEDF) and renal function in patients with diabetic retinopathy. *Mol. Vis.* **2008**, *14*, 992–6.
(52) Chen, C.; Tso, A. W.; Law, L. S.; Cheung, B. M.; Ong, K. L.; Wat, N. M.; Janus, E. D.; Xu, A.; Lam, K. S., Plasma Level of Pigment Epithelium-Derived Factor Is Independently Associated with the Development of the Metabolic Syndrome in Chinese Men: A 10-Year Prospective Study. *J. Clin. Endocrinol. Metab.* **2010**, *95* (11), 5074−81.
(53) Sabater, M.; Moreno-Navarrete, J. M.; Ortega, F. J.; Pardo, G.; Salvador, J.; Ricart, W.; Fruhbeck, G.; Fernandez-Real, J. M. Circulating pigment epithelium-derived factor levels are associated with insulin resistance and decrease after weight loss. *J. Clin. Endocrinol. Metab.* **2010**, *95* (10), 4720–8.
(54) Crowe, S.; Wu, L. E.; Economou, C.; Turpin, S. M.; Matzaris, M.; Hoehn, K. L.; Hevener, A. L.; James, D. E.; Duh, E. J.; Watt, M. J. Pigment epithelium-derived factor contributes to insulin resistance in obesity. *Cell Metab.* **2009**, *10* (1), 40–7.
(55) Szalai, A. J.; van Ginkel, F. W.; Wang, Y.; McGhee, J. R.; Volanakis, J. E. Complement-dependent acute-phase expression of C-reactive protein and serum amyloid P-component. *J. Immunol.* **2000**, *165* (2), 1030–5.
(56) Corrado, E.; Rizzo, M.; Coppola, G.; Fattouch, K.; Novo, G.; Marturana, I.; Ferrara, F.; Novo, S. An update on the role of markers of inflammation in atherosclerosis. *J. Atheroscler. Thromb.* **2010**, *17* (1), 1–11 .
(57) Hansson, G. K. Inflammation, atherosclerosis, and coronary artery disease. *N. Engl. J. Med.* **2005**, *352* (16), 1685–95.
(58) Jenny, N. S.; Arnold, A. M.; Kuller, L. H.; Tracy, R. P.; Psaty, B. M. Serum amyloid P and cardiovascular disease in older men and women: results from the Cardiovascular Health Study. *Arterioscler. Thromb. Vasc. Biol.* **2007**, *27* (2), 352–8.
(59) Bickerstaff, M. C.; Botto, M.; Hutchinson, W. L.; Herbert, J.; Tennent, G. A.; Bybee, A.; Mitchell, D. A.; Cook, H. T.; Butler, P. J.; Walport, M. J.; Pepys, M. B. Serum amyloid P component controls chromatin degradation and prevents antinuclear autoimmunity. *Nat. Med.* **1999**, *5* (6), 694–7.
(60) Yang, Q.; Graham, T. E.; Mody, N.; Preitner, F.; Peroni, O. D.; Zabolotny, J. M.; Kotani, K.; Quadro, L.; Kahn, B. B. Serum retinol binding protein 4 contributes to insulin resistance in obesity and type 2 diabetes. *Nature* **2005**, *436* (7049), 356–62.
(61) Graham, T. E.; Yang, Q.; Bluher, M.; Hammarstedt, A.; Ciaraldi, T. P.; Henry, R. R.; Wason, C. J.; Oberbach, A.; Jansson, P. A.; Smith, U.; Kahn, B. B. Retinol-binding protein 4 and insulin resistance in lean, obese, and diabetic subjects. *N. Engl. J. Med.* **2006**, *354* (24), 2552–63.
(62) Kloting, N.; Graham, T. E.; Berndt, J.; Kralisch, S.; Kovacs, P.; Wason, C. J.; Fasshauer, M.; Schon, M. R.; Stumvoll, M.; Bluher, M.; Kahn, B. B. Serum retinol-binding protein is more highly expressed in visceral than in subcutaneous adipose tissue and is a marker of intra-abdominal fat mass. *Cell Metab.* **2007**, *6* (1), 79–87.
(63) Jaconi, S.; Rose, K.; Hughes, G. J.; Saurat, J. H.; Siegenthaler, G. Characterization of two post-translationally processed forms of human serum retinol-binding protein: altered ratios in chronic renal failure. *J. Lipid Res.* **1995**, *36* (6), 1247–53.

(64) Jaconi, S.; Saurat, J. H.; Siegenthaler, G. Analysis of normal and truncated holo- and apo-retinol-binding protein (RBP) in human serum: altered ratios in chronic renal failure. *Eur. J. Endocrinol.* **1996**, *134* (5), 576–82.

(65) Tonjes, A.; Bluher, M.; Stumvoll, M. Retinol-binding protein 4 and new adipocytokines in nonalcoholic fatty liver disease. *Curr. Pharm. Des.* **2010**, *16* (17), 1921–8.

(66) Koch, A.; Weiskirchen, R.; Sanson, E.; Zimmermann, H. W.; Voigt, S.; Duckers, H.; Trautwein, C.; Tacke, F. Circulating Retinol-Binding-Protein 4 in critically ill patients before specific treatment: prognostic impact and correlation with organ function, metabolism and inflammation. *Crit. Care* **2010**, *14* (5), R179.

(67) Berdichevsky, A.; Guarente, L.; Bose, A. Acute oxidative stress can reverse insulin resistance by inactivation of cytoplasmic JNK. *J. Biol. Chem.* **2010**, *285* (28), 21581–9 .

(68) Al-Daghri, N. M.; Al-Attas, O. S.; Alokail, M.; Draz, H. M.; Bamakhramah, A.; Sabico, S. Retinol binding protein-4 is associated with TNF-alpha and not insulin resistance in subjects with type 2 diabetes mellitus and coronary heart disease. *Dis. Markers* **2009**, *26* (3), 135–40.

(69) Mitterberger, M. C.; Mattesich, M.; Klaver, E.; Lechner, S.; Engelhardt, T.; Larcher, L.; Pierer, G.; Piza-Katzer, H.; Zwerschke, W. Adipokine profile and insulin sensitivity in formerly obese women subjected to bariatric surgery or diet-induced long-term caloric restriction. *J. Gerontol., A: Biol. Sci. Med. Sci.* **2010**, *65* (9), 915–23.

(70) Lee, J. W.; Im, J. A.; Lee, H. R.; Shim, J. Y.; Youn, B. S.; Lee, D. C. Visceral adiposity is associated with serum retinol binding protein-4 levels in healthy women. *Obesity (Silver Spring)* **2007**, *15* (9), 2225–32.

(71) Haider, D. G.; Schindler, K.; Prager, G.; Bohdjalian, A.; Luger, A.; Wolzt, M.; Ludvik, B. Serum retinol-binding protein 4 is reduced after weight loss in morbidly obese subjects. *J. Clin. Endocrinol. Metab.* **2007**, *92* (3), 1168–71.

(72) Stefan, N.; Hennige, A. M.; Staiger, H.; Machann, J.; Schick, F.; Schleicher, E.; Fritsche, A.; Haring, H. U. High circulating retinol-binding protein 4 is associated with elevated liver fat but not with total, subcutaneous, visceral, or intramyocellular fat in humans. *Diabetes Care* **2007**, *30* (5), 1173–8.

(73) Daiger, S. P.; Schanfield, M. S.; Cavalli-Sforza, L. L. Group-specific component (Gc) proteins bind vitamin D and 25-hydroxyvitamin D. *Proc. Natl. Acad. Sci. U.S.A.* **1975**, *72* (6), 2076–80.

(74) Iyengar, S.; Hamman, R. F.; Marshall, J. A.; Majumder, P. P.; Ferrell, R. E. On the role of vitamin D binding globulin in glucose homeostasis: results from the San Luis Valley Diabetes Study. *Genet. Epidemiol.* **1989**, *6* (6), 691–8.

(75) Baier, L. J.; Dobberfuhl, A. M.; Pratley, R. E.; Hanson, R. L.; Bogardus, C. Variations in the vitamin D-binding protein (Gc locus) are associated with oral glucose tolerance in nondiabetic Pima Indians. *J. Clin. Endocrinol. Metab.* **1998**, *83* (8), 2993–6.

(76) Arnaud, J.; Constans, J. Affinity differences for vitamin D metabolites associated with the genetic isoforms of the human serum carrier protein (DBP). *Hum. Genet.* **1993**, *92* (2), 183–8.

(77) Kayaniyil, S.; Vieth, R.; Retnakaran, R.; Knight, J. A.; Qi, Y.; Gerstein, H. C.; Perkins, B. A.; Harris, S. B.; Zinman, B.; Hanley, A. J. Association of vitamin D with insulin resistance and beta-cell dysfunction in subjects at risk for type 2 diabetes. *Diabetes Care* **2010**, *33* (6), 1379–81 .

(78) Norman, A. W.; Frankel, J. B.; Heldt, A. M.; Grodsky, G. M. Vitamin D deficiency inhibits pancreatic secretion of insulin. *Science* **1980**, *209* (4458), 823–5.

(79) Tanaka, Y.; Seino, Y.; Ishida, M.; Yamaoka, K.; Yabuuchi, H.; Ishida, H.; Seino, S.; Imura, H. Effect of vitamin D3 on the pancreatic secretion of insulin and somatostatin. *Acta Endocrinol (Copenh.)* **1984**, *105* (4), 528–33.

(80) Winters, S. J.; Chennubhatla, R.; Wang, C.; Miller, J. J. Influence of obesity on vitamin D-binding protein and 25-hydroxy vitamin D levels in African American and white women. *Metabolism* **2009**, *58* (4), 438–42.

(81) Fish, E.; Beverstein, G.; Olson, D.; Reinhardt, S.; Garren, M.; Gould, J., Vitamin D Status of Morbidly Obese Bariatric Surgery Patients. *J. Surg. Res.* **2010**, *164* (2), 198−202.

(82) Harbottle, L., Audit of nutritional and dietary outcomes of bariatric surgery patients. *Obes Rev.* **2011**, *12* (3), 198−204.

(83) Carr, M. E. Diabetes mellitus: a hypercoagulable state. *J. Diabetes Complications* **2001**, *15* (1), 44–54.

(84) Franchini, M.; Lippi, G.; Manzato, F.; Vescovi, P. P.; Targher, G. Hemostatic abnormalities in endocrine and metabolic disorders. *Eur. J. Endocrinol.* **2010**, *162* (3), 439–51 .

(85) Antonio, J.; Street, C. Glutamine: a potentially useful supplement for athletes. *Can. J. Appl. Physiol.* **1999**, *24* (1), 1–14.

(86) Ratnayake, W. M.; Sarwar, G.; Laffey, P. Influence of dietary protein and fat on serum lipids and metabolism of essential fatty acids in rats. *Br. J. Nutr.* **1997**, *78* (3), 459–67.

(87) Stachlewitz, R. F.; Seabra, V.; Bradford, B.; Bradham, C. A.; Rusyn, I.; Germolec, D.; Thurman, R. G. Glycine and uridine prevent D-galactosamine hepatotoxicity in the rat: role of Kupffer cells. *Hepatology* **1999**, *29* (3), 737–45.

(88) Wheeler, M. D.; Ikejema, K.; Enomoto, N.; Stacklewitz, R. F.; Seabra, V.; Zhong, Z.; Yin, M.; Schemmer, P.; Rose, M. L.; Rusyn, I.; Bradford, B.; Thurman, R. G. Glycine: a new anti-inflammatory immunonutrient. *Cell. Mol. Life Sci.* **1999**, *56* (9−10), 843–56.

(89) Alarcon-Aguilar, F. J.; Almanza-Perez, J.; Blancas, G.; Angeles, S.; Garcia-Macedo, R.; Roman, R.; Cruz, M. Glycine regulates the production of pro-inflammatory cytokines in lean and monosodium glutamate-obese mice. *Eur. J. Pharmacol.* **2008**, *599* (1−3), 152–8.

(90) Greenfield, J. R.; Farooqi, I. S.; Keogh, J. M.; Henning, E.; Habib, A. M.; Blackwood, A.; Reimann, F.; Holst, J. J.; Gribble, F. M. Oral glutamine increases circulating glucagon-like peptide 1, glucagon, and insulin concentrations in lean, obese, and type 2 diabetic subjects. *Am. J. Clin. Nutr.* **2009**, *89* (1), 106–13.

(91) Lieber, C. S.; DeCarli, L. M.; Mak, K. M.; Kim, C. I.; Leo, M. A. Attenuation of alcohol-induced hepatic fibrosis by polyunsaturated lecithin. *Hepatology* **1990**, *12* (6), 1390–8.

(92) Costford, S. R.; Crawford, S. A.; Dent, R.; McPherson, R.; Harper, M. E. Increased susceptibility to oxidative damage in post-diabetic human myotubes. *Diabetologia* **2009**, *52* (11), 2405–15.

(93) Mate, A.; Miguel-Carrasco, J. L.; Monserrat, M. T.; Vazquez, C. M. Systemic antioxidant properties of L-carnitine in two different models of arterial hypertension. *J. Physiol. Biochem.* **2010**, *66* (2), 127–36 .

(94) Millington, D. S.; Kodo, N.; Norwood, D. L.; Roe, C. R. Tandem mass spectrometry: a new method for acylcarnitine profiling with potential for neonatal screening for inborn errors of metabolism. *J. Inherit. Metab. Dis.* **1990**, *13* (3), 321–4.

(95) Kim, J. Y.; Park, J. Y.; Kim, O. Y.; Ham, B. M.; Kim, H. J.; Kwon, D. Y.; Jang, Y.; Lee, J. H. Metabolic profiling of plasma in overweight/obese and lean men using ultra performance liquid chromatography and Q-TOF mass spectrometry (UPLC-Q-TOF MS). *J. Proteome Res.* **2010**, *9* (9), 4368–75.

(96) Adams, S. H.; Hoppel, C. L.; Lok, K. H.; Zhao, L.; Wong, S. W.; Minkler, P. E.; Hwang, D. H.; Newman, J. W.; Garvey, W. T. Plasma acylcarnitine profiles suggest incomplete long-chain fatty acid beta-oxidation and altered tricarboxylic acid cycle activity in type 2 diabetic African-American women. *J. Nutr.* **2009**, *139* (6), 1073–81.

(97) Frey, I. M.; Rubio-Aliaga, I.; Siewert, A.; Sailer, D.; Drobyshev, A.; Beckers, J.; de Angelis, M. H.; Aubert, J.; Bar Hen, A.; Fiehn, O.; Eichinger, H. M.; Daniel, H. Profiling at mRNA, protein, and metabolite levels reveals alterations in renal amino acid handling and glutathione metabolism in kidney tissue of Pept2−/− mice. *Physiol. Genomics* **2007**, *28* (3), 301–10.

(98) Weckwerth, W.; Wenzel, K.; Fiehn, O. Process for the integrated extraction, identification and quantification of metabolites, proteins and RNA to reveal their co-regulation in biochemical networks. *Proteomics* **2004**, *4* (1), 78–83.

(99) Perroud, B.; Lee, J.; Valkova, N.; Dhirapong, A.; Lin, P. Y.; Fiehn, O.; Kultz, D.; Weiss, R. H. Pathway analysis of kidney cancer using proteomics and metabolic profiling. *Mol. Cancer* **2006**, *5*, 64.

(100) Kuhner, S.; van Noort, V.; Betts, M. J.; Leo-Macias, A.; Batisse, C.; Rode, M.; Yamada, T.; Maier, T.; Bader, S.; Beltran-Alvarez, P.;

Castano-Diez, D.; Chen, W. H.; Devos, D.; Guell, M.; Norambuena, T.; Racke, I.; Rybin, V.; Schmidt, A.; Yus, E.; Aebersold, R.; Herrmann, R.; Bottcher, B.; Frangakis, A. S.; Russell, R. B.; Serrano, L.; Bork, P.; Gavin, A. C. Proteome organization in a genome-reduced bacterium. *Science* **2009**, *326* (5957), 1235–40.

(101) Paglialunga, S.; Fisette, A.; Yan, Y.; Deshaies, Y.; Brouillette, J. F.; Pekna, M.; Cianflone, K. Acylation-stimulating protein deficiency and altered adipose tissue in alternative complement pathway knockout mice. *Am. J. Physiol. Endocrinol. Metab.* **2008**, *294* (3), E521–9.

(102) Gorg, A.; Drews, O.; Luck, C.; Weiland, F.; Weiss, W. 2-DE with IPGs. *Electrophoresis* **2009**, *30* (Suppl 1), S122–32.